Atmos. Chem. Phys. Discuss., https://doi.org/10.5194/acp-2018-397
Manuscript under review for journal Atmos. Chem. Phys.
Discussion started: 10 August 2018

Atmospheric Chemistry and Physics Discussions

Impact of VOCs on the formation of ozone in a central China city during severe pollution periods

Bowei Li[1], Steven Sai Hang Ho[2,3*], Sunling Gong[1,4*], Jingwei Ni[1], Huairui Li[1], Liyan Han[1], Yi Yang[1], Yijin Qi[1], Dongxu Zhao[1]

[1] *Langfang Academy of Eco Industrialization for Wisedom Environment, Langfang 065000, China*

[2] *Division of Atmospheric Sciences, Desert Research Institute, Reno, Nevada, USA*

[3] *Key Lab of Aerosol Chemistry & Physics, Institute of Earth Environment, Chinese Academy of Sciences, Xi'an 710061, China*

[4] *Center for Atmosphere Watch and Services of CMA, Chinese Academy of Meteorological Sciences, Beijing 100081, China*

*Correspondence to: Steven Sai Hang Ho (stevenho@hkpsrl.org) and Sunling Gong (gongsl@cma.gov.cn)

Atmos. Chem. Phys. Discuss., https://doi.org/10.5194/acp-2018-397
Manuscript under review for journal Atmos. Chem. Phys.
Discussion started: 10 August 2018

Atmospheric Chemistry and Physics Discussions

Abstract

In this work, a five-month sampling campaign was conducted for volatile organic compounds (VOCs) for the first time in Zhengzhou City, Henan province, China, where ozone (O_3) pollution has shown an increasing trend in recent years. Fifty-seven VOCs defined by the Photochemical Assessment Monitoring Stations (PAMS) were sampled using canister method. Meanwhile, other O_3 precursor gases were monitored online at four different sites between the time period of May - September, 2017. The results indicated that the average mixing ratio of Σ_{PAMS} (31.57±23.35 ppbv) in Zhengzhou was lower than the other megacities in China, while alkyne was in a significantly higher proportion. The abundances, compositions and ratios of PAMS showed strong spatial and temporal variations. Alkenes were the largest contributors to the ozone formation potential (OFP). On clear days, higher O_3 levels were often accompanied with high Σ_{PAMS}/NO_x ratio at each site, demonstrating that the VOCs were more sensitive during the O_3 formation period in Zhengzhou. Furthermore, source apportionmemt was conducted with Positive Matrix Factorization (PMF) model, and it was found that the use of compressed natural gas (CNG), the evaporation of gasoline and the exhaust from vehicles were the important sources for ambient VOCs at all four sites. Besides, the meterological conditions and long-range transport from other surrounding provinces also had an impact on the air quality determined using the cluster analysis. It is worth mentioning that the reduction in VOCs' emissions is necessary to suppress the O_3 pollution.

1. Introduction

Volatile organic compounds (VOCs) are diverse and reactive chemicals. Vehicle exhausts, fuel combustion and evaporation, and solvent usage are the known major anthropogenic sources of VOCs (Zhang et al., 2014;Yan et al., 2017;Wang et al., 2013a;Liu et al., 2017;Sahu et al., 2017). Since VOCs play a crucial role in the formation of ground-level ozone (O_3) and secondary organic aerosol (SOA) (Yuan et al., 2013a;Han et al., 2018;Wang et al., 2018), studies on VOCs are being conducted globally (Wei et al., 2014;Malley et al., 2015;Ou et al., 2015;Zhu et al., 2017;Zhao et al., 2015). Fifty-seven VOCs, including C_2 - C_{10} alkanes, alkenes, alkynes and aromatics, which greatly

contribute to ambient O_3, have been defined and regularly monitored by Photochemical Assessment Monitoring Stations (PAMS) (Shao et al., 2016;Chen et al., 2010). With the rapid economic development, O_3 pollution has troubled all urban cities (Wang et al., 2017c;Nagashima et al., 2017). Non-linearity relationships between the ambient VOCs, nitrogen oxide (NO_x) and O_3 production indicate that the reduction in tropospheric O_3 is complex (Lin et al., 1998;Hidy and Blanchard, 2015;Li et al., 2018). During the time period of 1960 - 2010, the concentrations of VOCs and NO_x have decreased at the rate of 7.3% yr^{-1} and 2.6% yr^{-1}, respectively, due to which, the O_3 extrema declined in southern California (Pollack et al., 2013). Evaluations on the production efficiency of O_3 suggested the increase in responsiveness of O_3 to NO_x in southeastern U.S, and therefore, the changes in anthropogenic emissions of VOCs should be taken into consideration (Blanchard and Hidy, 2017). Many modeling and field studies proved that photochemical production of O_3 in several regions in China, such as Guangzhou, Shanghai and Beijing, were sensitive to VOCs (Shao et al., 2009;Gao et al., 2017;Ou et al., 2016), and the sensitivity regime was always in flux (Luecken et al., 2018). It is predicted that the formation regime of O_3 will be more sensitive to VOC emissions in China by 2030 (Jin and Holloway, 2015), On the other hand, the International Agency for Research on Cancer (IARC, 2017) has identified several VOCs, such as benzene and 1,3-butadiene as the first class carcinogens (Hoque et al., 2008;Iannuzzi et al., 2010).

In recent years, investigations involving the source apportionment of VOCs, acquirement of emission profiles and interpretation of the seasonal variations in China were mainly concentrated in Yangtze River Delta (YRD), Pearl River Delta (PRD) and Beijing-Tianjin region (BJT) (An et al., 2014;Wang et al., 2014;Chen et al., 2014;Liu et al., 2016a;Guo et al., 2017). With the nationwide deterioration of air quality, studies in less developed or developing regions, such as southwestern and northwestern China, are scarce. Contributions from the burning of biomass and high abundances of toxics and reactive compounds (such as, benzene) are prominent in these areas (Li et al., 2014;Li et al., 2017a). Consequently, differences on the structure and reactivity of VOCs, which render them different abilities to influence the production of ozone, and reactivity based on the air quality control measures, have developed (Capps et al., 2012). Additionally, U.S. Environmental Protection Agency (EPA) (2005) has encouraged states to take this approach while developing the

Ozone State Implementation Plans (OSIP). Aromatics and alkenes were responsible for most of the weighted reactivity of VOCs (59.4% and 25.8%, respectively) in PRD (Ou et al., 2015). With the changes in energy infrastructure, industrial construction and meteorological conditions (Wang et al., 2015;Shao et al., 2011), major emission sources of active compounds vary accordingly. For example, in less developed cities, such as Heilongjiang and Anhui, the combustion of biomass had the highest contribution to O_3 formation (40% and 36%, respectively), while in developed regions, such as Shanghai, Beijing and Zhejiang, the solvent use became more important with time (>20%) (Wu and Xie, 2017). Identifying the local chemical species play vital role in O_3 formation and provides useful information for policy-makers to make strategies to alleviate O_3 pollution.

Zhengzhou is an important developing city in the mid-west of Huanghe-Huaihe river flood plain in China. As the capital city of Henan province, it is densely populated with more than seven million residents in 2010 (Geng et al., 2013). With the rapid growth of industrial activities, vehicle emissions and fuel combustion, air quality in Zhengzhou has notoriously deteriorated. Zhengzhou is categorized as one of the most polluted cities due to the reason that on 65% of days in a year, its air quality exceeds the allowable limits set by Air Quality Guideline in 2013. The city has the third worst air quality among 74 nationwide cities in the first half year of 2015. Particularly, O_3 was the most critical pollutant in Zhengzhou in 65 - 85 days of summer (Shen et al., 2017;Gong et al., 2017). Over 50% of the days in a year, the mixing ratio of O_3 exceeded the Grade I standard of daily maximum average 8-hour (DMA8) (100 μg m^{-3}) in Henan, while the estimated mortality of chronic obstructive pulmonary disease (COPD), caused by O_3, was also higher compared to other provinces in China (Liu et al., 2018). As the major precursors of O_3, the study on VOCs is of significance. However, for the city of Zhengzhou (China), the related research is non-existent in literature. In this work, a comprehensive sampling campaign aiming at VOCs has been conducted at four monitoring stations during the time period of May - September 2017. The spatial and temporal variations in VOCs in Zhengzhou were determined. The contributions of major emission sources were quantified, and the relationship between O_3-VOCs-NO_x was discussed in detail. The results and implications from this study can provide useful guidance for policy-makers to alleviate ozone pollution in Zhengzhou, China.

Atmos. Chem. Phys. Discuss., https://doi.org/10.5194/acp-2018-397
Manuscript under review for journal Atmos. Chem. Phys.
Discussion started: 10 August 2018

Atmospheric Chemistry and Physics Discussions

2. Experimental

2.1 Sampling site

According to the population density and industrial facilities, and in combination with the prevailing southeastern wind, four sites have been selected for the sampling campaign. These sites are Jingkai community (JK; 113.73°E, 34.72°N), municipal environmental monitoring station (MEM; 113.61°E, 34.75°N), Yinhang school (YH; 113.68°E, 34.80°N) and Gongshui company (GS; 113.57°E, 34.81°N), which are located at the southeastern, southwestern, northeastern and northwestern of urban Zhengzhou, respectively (Fig. 1). There was a main airport highway and heavy-traffic ring roads approximately 500 m west of JK. Furthermore, the site was at a distance of 2 km from an industrial area, which involved packaging and printing plants, and material distribution factories. It is noteworthy that there were three coal power plants in the urban area of Zhengzhou city. One of the power plants with the highest production was 1.6 km northwest of MEM. Both the MEM and YH included a mix of commercial and condensed residential areas, whereas the apartments around YH were more aged. In addition, GS was surrounded by several manufacturing plants, including pharmaceuticals, materials, foods and machineries.

Ten sampling days with the rainfall record (*ca*. 0 mm) were chosen in every month during the period of May - September, 2017. Pre-evacuated stainless-steel canisters (Entech Instrument, Inc., Simi Valley, CA, USA), each having the volume of 3.2 L, were used to instantaneously collect VOCs. Two samples, one collected at 07:00 and the other at 14:00, were obtained on every sampling day. There were a total of 400 valid samples collected in this study. The chemical analysis was accomplished within two weeks after the collection of samples. Real-time data for trace gases, including SO_2, CO, NO_2 and O_3, and synchronous meteorological data, such as temperature (T), relative humidity (RH), wind direction (WD) and wind speed (WS), were recorded at each air monitoring station.

2.2 Chemical Analysis

In this study, the measurement of VOCs was based on Compendium Method TO-15, which was established by U.S. EPA. Air in the canister was concentrated using liquid-nitrogen at -160 °C

in a cryogenic pre-concentrator (7100A, Entech Instrument, Inc.). Both the CO_2 and H_2O were removed from the transfer line. The air was then thermally desorbed at 120 °C and transferred for analysis in a gas chromatography (GC, 7890A, Agilent Technologies, Santa Clara, CA, USA) coupled with mass spectrometric detector (MSD)/flame ionization detector (FID) (5977E, Agilent Technology). Dual columns and detectors were applied for the simultaneous analysis of C_2 - C_{11} hydrocarbons. A PLOT column with the length of 15 m, internal diameter of 0.32 mm and film thickness of 3.0 μm was connected to the FID for detection of C_2 - C_5 NMHCs, whereas C_5 - C_{10} NMHCs, oxygenated VOCs (OVOCs) and halocarbons were separated using a DB-624 (30 m × 0.25 mm inner diameter × 3.0 μm film thickness), which was connected to the MSD. The oven temperature of GC was programed to the initial temperature of 37 °C for 5 min, which was increased at the rate of 5 °C/min to 120 °C, and maintained at this temperature for 5 min. It was then ramped at the rate of 6 °C/min to the final temperature of 180 °C, where it was maintained for 5 min. The total run time was 41.6 minutes. The MSD was operated with the electron ionization (EI) impact (70 eV), where the ions were detected in the selected ion monitoring (SIM) mode. Based on the retention time and mass spectra involving accurate standard, the targeted VOCs were identified, and then, quantified using multi-point calibration curve. Three standard gases for TO-15 and PAMS (1 ppm; Spectra Gases Inc, NJ, USA) were used. A total of 101 compounds, including 28 alkanes, 11 alkenes, 17 aromatics, 34 halocarbons, 9 OVOCs, acetylene and CS_2 were quantified. This study discussed only 57 PAMS due to their critical role in O_3 pollution. Detailed information on the PAMS involved in this study and their corresponding linearity of calibration (R^2), measurement relative standard deviation (RSD), method detection limit (MDL), maximum increment reactivity (MIR, carter, 2010) are presented in Table 1.

2.3 Quality control and quality assurance (QC/QA)

QC/QA was thoroughly executed to ensure the quality of research and obtain trustworthy experimental data. In order to alleviate contamination from previous samples, canisters had to be repeatedly cleaned using humidified zero air before sampling. In order to inspect the cleanliness and vacuum in canisters, the pre-cleaned canisters, after storing for 24h, were analyzed using GC-MS according to the same analytical procedures used to analyze the field samples. The

canisters without any contamination were used for sampling. No obvious emission source was present during the sampling events. Daily calibration was performed using 2 ppbv standard mixtures to ensure the consistency and sensitivity of GC-MSD/FID system. The deviation in standard values was within ±20%. Abnormal QA/QC data with extremely high or low responses was recalibrated until the deviation was within the acceptable range.

2.4 Positive matrix factorization (PMF)

U.S. EPA PMF 5.0 was used for source apportionment (Liu et al., 2008b;Lau et al., 2010;Abeleira et al., 2017;Xue et al., 2017). Paatero and Tapper (1994) and Paatero (1997) thoroughly illustrated the rationale of PMF. Briefly speaking, PMF is a diagnostic method involving multivariate analysis, and involves decomposing the integrate sample data into two matrices, namely the source profiles and the source contributions. The method takes advantage of other observation data, such as wind direction and speed. The analyst could get messages on major emission sources, which contribute to ambient VOCs. Detailed information on the application of PMF can be referred to the publications cited above and to the PMF 5.0 user manual (U.S. EPA, 2014).

Based on the chemical mass balance between the input concentrations and the chemical profiles, PMF regarded the ambient data x_{ij}, namely the concentration of j^{th} constituent in i^{th} sample, as the gross values contributed by p sources according to Eq. (1).

$$X_{ij} = \sum_{k=1}^{p} g_{ik} f_{kj} + e_{ij} \quad (1)$$

where g_{ik} stands for the contribution of k^{th} factor in the i^{th} sample , while f_{kj} is the load of j^{th} compound in the k^{th} source. Furthermore, e_{ij} is the relevant residual.

In order to avoid negative source contributions, penalty function was adopted for constraints. Each data point can be individually weighed in the model, while the samples with lots of missing values were excluded.

Atmos. Chem. Phys. Discuss., https://doi.org/10.5194/acp-2018-397
Manuscript under review for journal Atmos. Chem. Phys.
Discussion started: 10 August 2018

Atmospheric Chemistry and Physics Discussions

Based on the algorithm on uncertainties (U), expressed as Q values, the stability of running results was assessed according to Eq. (2).

$$Q = \sum_{i=1}^{n}\sum_{j=1}^{m}\left[\frac{x_{ij} - \sum_{k=1}^{p} g_{ik} f_{kj}}{u_{ij}}\right]^2 \quad (2)$$

where u_{ij} stands for the uncertainty of the j^{th} compound in i^{th} sample.

In the PMF model, uncertainty is a function to evaluate the deviations in sampling and analysis procedure (Paatero, 2007). The uncertainty (U) can be calculated based on Eq. (3) (Polissar et al., 1998).

$$U = \begin{cases} \sqrt{(EF \times concentration)^2 + (MDL)^2} & (\text{conc.} > \text{MDL}) \\ \frac{5}{6} MDL & (\text{conc.} \le \text{MDL}) \end{cases} \quad (3)$$

where EF signifies the error fraction that equals 100 times of the percentage uncertainty.

3 Results and discussion

3.1 Mixing ratios and meteorological variations

The total concentrations of PAMS (Σ_{PAMS}) were different for all four sites (Table 2), and the ranks were inconsistent between each sampling month. In May 2017, the highest Σ_{PAMS} was reported at JK (37.65±22.58 ppbv), followed by GS (31.73±18.70 ppbv), YH (30.05±16.43 ppbv) and MEM (29.05±15.34 ppbv), while the Σ_{PAMS} values for the month of June, July, August and September were found to be in the order of: GS>JK>MEM>YH, MEM>GS>JK>YH, YH>MEM>JK>GS, and MEM> YH > GS >JK, respectively. Beside the emission sources (to be discussed in Section 3.2), the meteorological conditions also contributed to the variations. For instance, the prevailing wind in May was northwestern at MEM, GS and YH, while the southwestern wind was dominant at JK. The transportation of air pollutants from urban center and industrial plants meant that the highest level of Σ_{PAMS} was seen at JK. In June 2017, the prevailing wind vector changed to southeastern at MEM and GS. The average wind speed at GS (0.74±0.33 m s^{-1}) was significantly lower than that at MEM (1.84±0.94 m·s^{-1}), indicating poor dispersion

199 conditions at GS. Furthermore, the air pollutants emitted from MEM were more accumulated at GS,
200 which was due to higher Σ_{PAMS} at GS (39.29±25.37 ppbv) than that at MEM (30.28±12.77 ppbv).
201 It should also be noted that, when Σ_{PAMS} at JK was higher than that of GS, the levels at YH were
202 higher than those of MEM, and vice versa. Based on their geographic locations, both the GS and
203 MEM were located in the western part of Zhengzhou city, while JK and YH were situated in the
204 eastern side of the city. Except for the discriminations between the pollution sources at every site,
205 the above phenomenon might be a result of topographical effect.

206 C_2 - C_5 alkanes, acetylene, ethylene, toluene and benzene were the most abundant PAMS
207 detected at all sites (Table 3). These chemicals had the contribution of >60% for Σ_{PAMS},
208 representing the general consistency of pollution sources in the region. The mixing ratios of toluene
209 varied within a wide range at each site. Toluene is an important aromatic and has a variety of
210 emission sources (Wang et al., 2014;Barletta et al., 2005), among which, the vehicle exhaust and
211 solvent usage are the major contributors. Due to variable origins and emission strengths, few
212 compounds exhibited wide ranges in certain months. The mixing ratios of cyclohexane, isopentane,
213 toluene, and isobutane had large deviations at MEM in June, which were attributed to the increase
214 in liquefied petroleum gas (LPG) and gasoline evaporation due to the increase in ambient
215 temperatures (Li et al., 2017a;Liu et al., 2008a). At YH and GS, the largest deviations were seen in
216 the month of September. The mixing ratios of fossil fuel combustion markers, such as acetylene
217 (5.08±8.36 ppbv), toluene (4.37±5.28 ppbv), and m,p-xylene (1.09±1.62 ppbv) were varied
218 significantly at YH (Zheng et al., 2017). The variations in propane (10.77±17.73 ppbv), n-butane
219 (7.55±13.79 ppbv), isobutane (5.46±10.76 ppbv) and isopentane (5.25±8.76 ppbv) at GS were
220 reasonably significant due to the evaporation of gasoline and the use of LPG (Li et al., 2017a;Liu et
221 al., 2008a). Both cases demonstrate the widespread combustion sources and fuel evaporation in
222 Zhengzhou city.

223 Among these organic classes, alkane was the most abundant (Fig.2), and accounted for
224 52.85%, 62.52%, 53.38%, 53.39% of the total Σ_{PAMS} values at JK, MEM, GS, and YH, respectively.
225 The highest composition of alkane was observed at MEM due to the stronger contributions of
226 ethane, iso-pentane and other branched alkanes (such as, the ones having carbon number of 7 - 8).

Wang et al. (2017b) reported that these compounds could originate from the cooking process, which is consistent with the results reported here, as there was a shopping mall with a number of canteens around 200 m northeast to the sampling station. In addition, many restaurants were also scattered around.

In comparison, the aromatic compounds showed lower compositions in the afternoons (for example, around 14:00 LT) than the mornings (for example, around 07:00 LT) (Fig. 2). Increases in alkene compositions were mainly ascribed to higher contributions of isoprene, which was emitted from biogenic sources at higher temperature and solar irradiation. Isoprene's contribution to Σ_{PAMS} value at JK at was 12% at 14:00 LT (Fig.2), which was much higher than the other three sites. These results are in accordance with its larger vegetation coverage in the surrounding areas.

The average Σ_{PAMS} values in Zhengzhou city was significantly lower than those in Beijing (65.55 ppbv), Hangzhou (55.9 ppbv), Guangzhou (47.3 ppbv) and Nanjing (43.5 ppbv), though they were higher than that in Wuhan (23.3±0.5ppbv) (Guo et al., 2012;Li and Wang, 2012;An et al., 2014;Lyu et al., 2016;Raysoni et al., 2017). Furthermore, population density, industrial activity, fuel composition, local stringent regulations for environmental protection, terrain, and weather contributed to their abundances. Alkanes were generally the largest contributor in most areas (Fig. 2), while the compositions of aromatics were relatively lower in Zhengzhou city. It is well known that aromatics mainly originate from solvent usage and vehicle exhaust. It is also worth mentioning that Zhengzhou has less manufacturer involved in shoemaking and shipbuilding than Guangzhou and Nanjing. The registered number of vehicles was also lower than that in Beijing. On the other hand, higher composition of alkyne was observed in Zhengzhou. Alkyne typically originates from combustion sources. Henan is the largest agricultural province in China. As the sampling duration covered the crop harvest in June, the residents often used crop residues as the biofuel for their subsistence, thus resulting in higher alkyne compositions.

3.2 Temporal variations

The time series of mixing ratios of CO, SO_2, NO, NO_2, O_3 and PAMS at every site are shown in Fig. 3. Both the *T* and *RH* are also included in Fig. 3. The results showed that there is a

distinctive temporal characteristic, during which, lower levels of all air pollutants were observed in July and August (mid-summer) than in other months. These results were similar to those obtained for other urban areas (Li and Wang, 2012;Cheng et al., 1997;Na et al., 2001). Changes in boundary layer depth, human activities, and abundance of hydroxyl radicals (•OH) were the potential causes for the phenomenon. Pal et al.(2012) reported that the height of atmospheric boundary layer was positively correlated with temperature. In the current study, the highest ambient temperature was observed in July, while the occurrence of precipitation was more frequent in most areas of China during this period. Furthermore, stronger dispersion efficiently offered a wash-out effect for diluting the air pollutants to lower levels in ambient air. Additionally, a series of effective local policies, such as prohibition of painting and coating in open air and limitations on fuel supply between 10:00 -17:00 LT during hot summer days assisted in suppressing the VOCs' emissions. Meanwhile, many organizations, such as schools, institutes and scattered private workshops, were closed due to summer vacations. Some large-scale industries also stopped manufacturing processes for two weeks during this period. Due to this, the anthropogenic emissions reduced, which in turn resulted in a decrease in VOCs, SO_2, and NO_x emissions. The reduction of precursor levels and unfavorable photochemical conditions (such as, higher RH and WS) resulted in the O_3 levels to be constantly below the standard.

As demonstrated in Fig. 3, the observed Σ_{PAMS} values at 07:00 LT were often higher than those at 14:00 LT. The accumulation of pollutants during night-time and the temperature inversion in the morning were the most reasonable explanations for this phenomenon. Stronger photochemical reaction during noon-time led to the reduction in atmospheric VOCs. It should be noted that pronounced Σ_{PAMS} were occasionally observed at MEM and GS, which were potentially ascribed to sharp changes in local emissions and meteorological conditions. At MEM, the distinctive increment was always accompanied by obvious uplift of alkanes or aromatics. Combined with the changes in other parameters, such as levels of NO, NO_2, SO_2, CO, RH and T, it was concluded that the abnormally high Σ_{PAMS} values at MEM were mainly caused by enhanced combustion sources. Due to the disturbance from solvent use for building renovation, extremely high levels of aromatics were observed at GS in June. In addition, there were potential impacts from gas-fueled power

282 plants, which were located about 1 km northwest of the site. Compressed natural gas (CNG) or
283 LPG consumptions resulted in an increase in mixing ratio of propane, isobutane and n-butane
284 (Huang et al., 2015b), which was found consistent with the observations at this site.

285 Acetylene is a stable chemical compound that mainly originates from the combustion of
286 biomass/fossil fuel. On the morning of 5th September (highlighted in pink in Fig. 3), alkyne was
287 found in extremely high concentrations (14.65 - 39.42 ppbv). Its mixing ratio in most of the urban
288 areas was <10 ppbv (Louie et al., 2013;Duan et al., 2008;Guo et al., 2012). It was learnt that the 5th
289 September is a festival day for the people, who worship their ancestors. A large number of incenses
290 and offerings, made up of wood and paper, were burnt during the festival, resulting in an increase in
291 the mixing ratio of acetylene all over the Zhengzhou city.

292 **3.3 Spatial variations**

293 Average Σ_{PAMS} were higher at industrially impacted sites of GS (31.66±28.73 ppbv) and JK
294 (28.63±22.04 ppbv) than those at the other two sites (MEM and YH). Additionally, the air
295 pollutants related to the combustion process, such as SO_2 and CO were also in abundance in
296 western area of Zhengzhou (GS and MEM), where stronger emission sources were related to the
297 combustion of biomass or fossil fuel. Meanwhile, the O_3 levels did not present the same trend with
298 Σ_{PAMS} among the four sites, indicating that the transformation between O_3-NO_x-VOCs was more
299 complex than the linear reactions.

300 In June, the O_3 concentration often exceeded the national standard level of 80 ppbv. The
301 average mixing ratio of O_3 during daytime (07:00-18:00 LT) at JK, MEM, YH, and GS were 74.87
302 ±39.55 ppbv, 73.50±40.59 ppbv, 73.81±35.69 ppbv, and 87.99±46.11 ppbv, respectively. The
303 order of these values is consistent with that of the Σ_{PAMS}, in which the higher levels were observed
304 at JK and GS. Combined with the higher solvent usages, highest aromatics levels and the severer O_3
305 pollutions were found at GS as expected. Even though both the Σ_{PAMS} and higher O_3 formation
306 potential compounds (such as, alkenes and aromatics) at MEM were a bit higher than those at YH,
307 a reverse order of O_3 concentration was observed. Such phenomenon could be attributed to other
308 critical precursors, such as NO_x, which are involved in the formation of O_3. NO at MEM (8.48±

309 25.74 ppbv) was significantly higher than that at YH (2.57±3.08 ppbv) during daytime, indicating
310 that the reaction between O_3 and NO was more efficient at MEM.

311 It is well known that O_3 pollution is a regional problem. Streets et al. (2007) reported that the
312 contribution of air pollutants, derived from Hebei, was around 35 - 60% to the pollution in Beijing,
313 which experienced O_3 episodes. Along with the decrease in ambient temperature and light intensity,
314 and an increase in RH, the number of non-attainment O_3 days theoretically reduced after June, 2017,
315 while the maximum was observed on August 10th, 2017 (highlighted in yellow in Fig. 3). VOCs are
316 the critical contributors to the formation of O_3. The reductions in Σ_{PAMS} in the afternoons (around
317 14:00 LT) compared to mornings (around 07:00 LT) may have originated from the uptake by O_3
318 formation (Fig. 4). Furthermore, the highest VOCs concentration was observed at YH, which was
319 due to its downwind position to the other three sites between 08:00 - 15:00 LT on August 10th (Fig.
320 4). Additionally, the transmission of pollutants led to an abnormally high O_3 level at YH.

321 Overall, when the synoptic conditions, such as *T*, *RH* and *WS* were favorable, the O_3 level was
322 accompanied by the increase in VOCs concentrations, which potentially demonstrated that the O_3
323 formation was more sensitive to the abundance of VOCs in Zhengzhou city.

324 **3.4 Ratios of specific compounds**

325 Ratios of specific VOCs are useful indicators to identify the emission sources (Raysoni et al.,
326 2017;Liu et al., 2015;Li et al., 2017c;Huang et al., 2017;Ho et al., 2009). In order to characterize
327 the differences in the contribution of various sources at each site, two ratios of toluene/benzene and
328 i-pentane/n-pentane were discussed. The ratio of toluene to benzene (T/B) is an efficient tool to
329 differentiate between pollution sources, such as vehicle exhaust, coal combustion and solvent use
330 (Sun et al., 2018). As shown in Fig. 5, the T/B ratio showed variation during days and months. In
331 addition, the correlations between toluene and benzene were different throughout the sampling
332 period, indicating that their emission sources were always changing. The atmospheric lifetimes for
333 toluene and benzene are 1.9 days and 9.4 days, respectively, while the abundance of •OH was
334 assumed to be 10^6 rad cm^{-3} (Monod et al., 2001). Therefore, toluene was consumed more rapidly
335 than benzene during the photochemical reaction. Due to this reason, the T/B ratios at 14:00 LT

were almost lower than those at 07:00 LT. However, in September, higher T/B ratios at 14:00 LT were observed more frequently at MEM and YH than the other station. Meanwhile, the values were increased regionally, which was in accordance with the weaker photochemical reactions in late summer.

The R^2 value for the correlation between benzene and toluene was better in May (0.73 - 0.84) than during other months for all sites, and the average ratio in this month varied within the range of 1.81 - 3.36 for all four sites. Both the tunnel studies and roadside researches indicated that T/B ratio varied within the range of 1 - 2 when the atmosphere was heavily impacted by vehicle emissions (Gentner et al., 2013;Tang et al., 2007;Huang et al., 2015b;Wang et al., 2002). When the ratio was less than 0.6, it may be due to other sources, such as coal combustion and biomass burning (Tsai et al., 2003;Akagi et al., 2011). The industrial activity becomes more important when the value of T/B ratio is higher than 3 (Zhang et al., 2015). The results suggest that evident impacts were observed from vehicle emissions on the T/B ratio during the sampling period. Except for September, the average T/B ratio at JK lied within the range of 1.47 - 2.72, which was due to the vehicle emissions. Due to less interruption from photochemical reaction, the impact from industrial activities, which were mainly related to industrial clusters composed of automotive–related workshops and printing shops, and located approximately 2 km southwest of the observation site became important and resulted in higher T/B value (3.89) in September at JK. It is apparent that the T/B ratio at MEM was on the low side during the period of May - August (0.96 - 1.68), highlighting the impact of coal-fired thermal power plant. After excluding the abnormal values, the average ratio at GS (0.44 - 1.17) exhibited clear characteristics related to the combustion of coal/biomass during the period of June - August. This was related to the fact that the region was located on the edge of Zhengzhou. The impacts from biomass burning would be heavier than in other areas during the harvesting season. On the other hand, the coal fired power plant next to SZ was located at the southeast of GS with the linear distance of 5 km between the two points. Considering that the prevalent wind direction was southeastern during the period of June - August, the air pollutants emitted from the power plant could be easily transported to this region. Overall, the emission sources related to industrial activities were more evident in September. It is likely that the traffic emissions at JK and

combustion sources related to coal or biomass at MEM and GS would account for more contributions to VOCs, while there were no consistent results observed for YH due to the wide span of T/B ratio (1.07 - 5.38).

i-Pentane has similar reactivity to n-pentane (Jobson et al., 1998). The ratio between these two VOCs is useful in differentiating the potential sources, such as natural gas drilling and vehicle emissions. In this study, i-pentane and n-pentane were highly correlated (R^2=0.78 - 0.89) throughout the whole sampling campaign (Fig. 6), indicating stable sources for these two compounds. In the area, heavily impacted by natural gas drilling, the ratios lied within the range of 0.82 - 0.89 (Gilman et al., 2013;Abeleira et al., 2017). Higher values were often reported for automobiles, such as 2.2 - 3.8 for vehicle emissions, 1.8 - 4.6 for fuel evaporation, and 1.5 - 3.0 for gasoline (Russo et al., 2010;McGaughey et al., 2004;Jobson et al., 2004;Wang et al., 2013b). Low values within the range of 0.56 - 0.80 were found for coal combustion. The highest ratio was observed at JK (2.73), which was comparable to the value of 2.93 reported in a Pearl River Tunnel (Liu et al., 2008a), thus indicating strong impacts from traffic-related sources. The average ratio at MEM (2.02) was inconsistent with the characteristics of coal combustion. Yan et al. (2017) reported that the ratio for areas, which include several coal-fired thermal power plants, was approximately 0.55. The variation could be explained by factors, such as production scales, fuel compositions, sampling time and terrain. Additionally, it is remarkable that MEM was surrounded by a main road with four traffic lanes. The distance between the nearest traffic light and the sampling site was just 200 m. Frequent idling may cover up the contribution from coal combustion, thus overshadowing the effect of traffic emissions. The average ratio at GS (1.85) was close to that at YH (1.68). This was due to the similarity between the traffic related sources (such as, gasoline and fuel evaporation). The results showed that the vehicle emissions were an important source for VOCs in Zhengzhou city.

3.5 Reactive chemicals

Due to large differences in the reactivity of individual species, the contribution of each component to O_3 formation was different. Ozone formation potential (OFP) is a useful tool to

identify local active species that contribute the most to O_3 pollution (Huang et al., 2017). OFP is calculated using Eq. (4).

$$OFP=C_i \times MIR \quad (4)$$

where C_i represents the concentration level of i^{th} species, while *MIR* is a constant taken from Carter (2010) (Table 1).

Different from the results reported by (Wu and Xie, 2017), based on the emission inventory for North China Plain (NCP), YRD and PRD, where the largest contributor was the aromatics, followed by alkenes, alkenes were the most significant contributors (55.91±14.17%) to the sum of OFP in Zhengzhou city. The biggest contributors included ethylene, isoprene, m,p-xylene, toluene, propylene, acetylene, n-butane, i-pentane and propane, and their contributions lied within the range of 74.64 - 79.90% of the sum of OFP (Table 5). The composition of acetylene was higher compared to other areas (Li and Wang, 2012;Jia et al., 2016), demonstrating that it is necessary to conduct emission controls on sources related to combustion in Zhengzhou city.

It is well known that the ratio between VOCs and NO_x is an important index to analyze variable O_3 concentrations (Toro et al., 2006;Simon et al., 2015;Geng et al., 2009;Jin and Holloway, 2015;Geddes et al., 2009;Li et al., 2017b). Zhengzhou suffered from the severest O_3 pollution in June, 2017. The relationships between OFP of each organic group, Σ_{PAMS}, and the concentrations of NO_x and O_3, as well as the corresponding meteorological conditions, are shown in Fig. 7. At every site at 07:00 LT, WS was generally lower than that at 14:00 LT, indicating weaker vertical distribution. With the lower RH and higher T and OFP (88.13±30.32 ppbv) values, lower O_3 was unexpectedly seen at YH than MEM on sunny days, which was attributed to lower Σ_{PAMS}/NO_x ratios at YH (highlighted in pink in Fig. 6). The total OFP was higher at JK than at other sites, although the actual O_3 levels at JK were very close to those at MEM and even lower than those at GS. A lower WS at GS (0.65±0.26 m s^{-1}) promoted the pollutant accumalation The ratio of Σ_{PAMS}/NO_x was more scattered at JK and MEM than at YH and GS along with the variable WS, thus demonstrating significant impacts from metelogical conditions. During clear days, higher O_3

concentration was always accompanied by higher Σ_{PAMS}/NO_x ratio at each site, indicating a close relationship between the Σ_{PAMS}/NO_x ratio and O_3.

3.6 Source apportionment

In order to select appropriate chemical species for PMF model, following principles were used. Species with mixing ratios usually below MDL were eliminated. Except for the source markers, species with high reactivity should be excluded (Shao et al., 2016;Guo et al., 2011). Finally, 28 VOC species and NO_2 were chosen for the source analysis. Q(robust), Q(true) and Q(true)/Q(exp) are presented in Table 6. Based on the model results, seven factors were defined at MEM, YH, and GS, while eight factors were defined at JK (Fig.8).

Source profiles showed that the sites had similar regional characteristic. There was a strong common source (factor 1) for C_2 - C_5 n-alkanes and certain amounts of C_2 - C_4 alkenes, benzene, toluene, acetylene and NO_2.It is reported that i-Pentane and aromatics (such as, benzene, toluene, ethylbenzene and m/p-xylene) usually originated from gasoline evaporation, while isobutane and n-butane were emitted from LPG/CNG usage (Li et al., 2017a;Liu et al., 2008a). Considering the wide consumption of CNG for residential cooking in Zhengzhou, this factor was defined as CNG+gasoline evaporation.

The second factor was characterized based upon significant loading of toluene, ethylbenzene, m/p-xylene, and 1,2,4-trimethylbenzene. According to previous studies (Yuan et al., 2010;Wang et al., 2014), toluene and C_8 - C_9 aromatics were the major VOCs emitted from paint applications. Therefore, Source 2 was assigned as the solvent use. This is consistent with the real situation that there were widespread road paving and building constructions in Zhengzhou city. In addition, car decoration, printing, and furniture manufacturing, which are associated with the use of adhesives, were also included in this source category.

The third source was associated with the significant portion of long chain alkanes (C_7 - C_9) and high amounts of toluene, which are tracers for diesel evaporation (Liu et al., 2008a). Therefore, Source 3 was identified as the diesel vapor. Beside on-road vehicles, many non-road mobile machineries used for building or railway station constructions were correlated with this source.

444 Source 4 was dominated by trans-2-butene and 1-butene. These species were mainly produced
445 in coal combustion (Liu et al., 2008a;Yan et al., 2016). Liu et al. (2016b) reported that 1-butene
446 was a critical VOC generated during the smoldering process of coal combustion. This factor was
447 thus categorized as the coal combustion.

448 The fifth factor shows a dominant loading of cyclohexane, methylcyclohexane, styrene,
449 2-methylhexane and 3-methylhexane. The first three VOCs were identified as the components
450 heavily impacted by petrochemical industries (Jobson et al., 2004). Therefore, this source was
451 defined as the petrochemical.

452 Source 6 was composed of ethylene, propylene, benzene, toluene, 3-methylpentane, n-heptane,
453 acetylene and NO_2. In urban areas, vehicle emissions are a major source for ethylene and propylene
454 (Wang et al., 2017a). Fossil fuel combustion produces large amounts of acetylene (Ho et al., 2009),
455 while NO_2 is a typical tracer for vehicle exhaust (Huang et al., 2015a). The source was referred to
456 as the vehicle exhaust.

457 Source 7 was distinguished by extremely high compositions of isoprene, a species mainly
458 produced by vegetation through photosynthesis (Millet et al., 2016). Even though, it can be emitted
459 from traffic-related sources (Yuan et al., 2009), this possibility can be ignored by its poor
460 correlations with other source makers of vehicle exhaust (such as, i-pentane and ethylene).
461 Therefore, this source was identified as the biogenic emissions.

462 Factor 8 was only resolved for the JK site. The major compounds present in this source were
463 ethylene, propylene, acetylene and NO_2. These compounds mainly originated from on-road vehicles
464 (Wang et al., 2017a). Since there were minor contributions of alkanes and aromatics, they were
465 possibly derived from on-road vehicles under different running conditions. This factor was named
466 as the traffic-related source.

467 According to the source apportionment results (Fig. 9), CNG usage, gasoline evaporation and
468 vehicle exhaust had considerable portions and were the important sources for ambient VOCs at
469 every site. The smallest contribution from CNG and gasoline evaporations was found at GS
470 (24.99%), which was lower than the values observed at JK (35.06%) and YH (34.28%), and was

probably caused by the heavier traffic at JK and larger consumption of CNG (from the condensed canteens and active household cooking) at YH. The distribution of petrochemical source was uneven on the regional scale, with the largest portion observed at MEM (11.56%) and comparable values found for JK (3.44%), YH (6.21%) and GS (5.56%). These results are in accordance with the fact the distance between the petrochemical plants and the sampling site of MEM was the shortest (*ca.* 2 km). The weighted percentages attributed to the solvent use were similar among the four sites, with the highest value of 12.41% at MEM, which was consistent with the fact that there was less abundance of aromatics in Zhengzhou city. The emission source related to diesel fuel was more evident at JK (11.76%). The area was rife with logistics companies and frequently suffered from disturbance of heavy-duty cargo vehicles powered by diesel fuel. Coal combustion impacted the ambient air heavily at MEM (17.84%) and GS (13.50%), which were only 2 km and 5 km away from the thermal power plants, respectively. Overall, the traffic-related source was the most important emission source for VOCs in Zhengzhou, which is in accordance with the results obtained for other urban areas (Yuan et al., 2013b;Lyu et al., 2016;Lau et al., 2010).

3.7 Long-range transport

Air transported from surrounding areas had impacts on the air quality at the study site (Langford et al., 2010;Sun et al., 2018). In this work, Hybrid Single-Particle Lagrangian Integrated Trajectory (HYSPLIT) model was used to present the long-range transport effects on the air quality of Zhengzhou city (Fig. 10). Meteorological conditions are important factors that impact both the compositions and levels of VOCs. Clusters arriving at Zhengzhou in May, 2017 demonstrated longer paths, and included six clusters in total. The largest one (27.2%) was originated from Yinchuan city, which is a central city in northwest China. The cluster passed over several non-capital cities (such as, Yanan, Yuncheng and Luoyang) in Shanxi and Sichuan provinces. Such long-range transportation of pollutants might have less impact on the air quality of Zhengzhou, which agrees well with the comparable levels and similar compositions of VOCs during the period of May - June. In the months of June, August and September, approximately half of the air currents originated from the areas of Henan province. The air current originating from Hubei province took up the largest portion (*ca.* 88.68%) of clusters in July, and potentially led to a significant variation

in the concentration or composition of VOCs. As illustrated in Fig. 2, the average concentration level of Σ_{PAMS} in July sharply decreased to 15.91±6.54 ppbv. This was accompanied by the weighted percentage of aromatics, which dropped to 10.30±4.23%. It is well known that alkenes and aromatics have high photochemical reactivity. The T/B ratio also showed the lowest level (1.15±0.99) around this period, illustrating that the air plumes had longer lifetime. Both of these evidenced that Zhengzhou was impacted by air pollutants, which originated from Hubei province. According to previous studies in Wuhan, the capital city of Hubei province, the average total Σ_{PAMS} (23.3±0.6 ppbv) (Lyu et al., 2016) was much lower than the average level in Zhengzhou (31.57±23.35 ppbv). The cleaner air mass clusters, originating from Hubei in July, can thus be designated as a dilute flow.

4. Conclusions

In this study, PAMS were collected at four different sites in Zhengzhou, Henan (China) for the first time. C_2 - C_5 alkanes, acetylene, ethylene, toluene and benzene were the most abundant VOCs in the region. On the basis of monthly average, the maximum Σ_{PAMS} was observed at GS, which was impacted by various emission sources. In comparison to other Chinese cities, the weighted percentage of aromatics was lower, while higher alkyne level was observed in Zhengzhou city. Due to less anthropogenic emissions and more favorable dispersion conditions, most of the air pollutants had the lowest levels in the mid-summer month of July. Overall, the O_3 levels were correlated with Σ_{PAMS}, which potentially demonstrated that the O_3 formation was more sensitive to the abundance of VOCs in Zhengzhou. Different from other megacities, alkenes were the biggest contributors to OFP, while acetylene was particularly critical at each site. The CNG usage, gasoline evaporation and vehicle exhaust were the important sources for ambient VOCs. Cleaner air clusters from Hubei occasionally arrived at Zhengzhou. This study provides the first-hand information on the characteristics of VOCs and assists in overcoming the O_3 pollution issue in Zhengzhou city, China.

Acknowledgements

This research was supported by the Key Program of National Natural Science Foundation of China (Grant No. 91744209).

Atmos. Chem. Phys. Discuss., https://doi.org/10.5194/acp-2018-397
Manuscript under review for journal Atmos. Chem. Phys.
Discussion started: 10 August 2018

Atmospheric Chemistry and Physics Discussions

527 **Table & Figure**

528 Table1. Detailed information on the calibration curve for 57 PAMS and their MIR

	Species	R^2	MDL(pptv)	RSD	MIR		Species	R^2	MDL(pptv)	RSD	MIR
	Ethane	0.9998	6.8	5%	0.28		Ethylene	0.9997	12.5	10%	9
	Propane	0.9998	2.8	2%	0.49		Propylene	0.9998	6.2	5%	11.66
	Isobutane	0.9998	3.2	3%	1.23		Trans-2-butene	1	3.6	6%	15.16
	n-Butane	0.9998	6.7	5%	1.15		1-Butene	0.9995	7.8	6%	9.73
	Cyclopentane	0.9971	8.5	7%	0.09		Cis-2-butene	0.9997	6.8	6%	14.24
	Isopentane	0.9999	5.5	4%	0.93	**Alkene**	1,3-butadiene	0.9874	13.5	8%	
	n-Pentane	0.9999	6.6	5%	0.88		1-Pentene	0.9764	6.3	5%	7.21
	2,2-Dimethyl-butane	0.9963	5.4	4%	1.17		Trans-2-pentene	0.9964	10.1	7%	10.56
	2,3-Dimethylbutane	0.9966	7.6	6%	0.97		Isoprene	0.9966	7.7	6%	10.61
	2-Methylpentane	0.9958	8.0	6%	1.5		Cis-2-pentene	0.9965	8.6	7%	10.38
	3-Methylpentane	0.9967	5.4	4%	1.8		1-Hexene	0.9961	11.4	9%	4.4
Alkane	n-Hexane	0.9967	7.3	6%	1.24	**Alkyne**	Acetylene	0.9996	7.1	5%	0.95
	2,4-Dimethylpentane	0.9972	9.6	7%	1.55		Benzene	0.9975	6.5	5%	0.72
	Methyl-cyclopentane	0.9974	5.8	5%	2.19		Toluene	0.9963	4.3	4%	4
	2-Methyl-hexane	0.9968	8.6	7%	1.19		Ethyl-benzene	0.9955	4.8	4%	3.04
	Cyclohexane	0.9958	7.7	6%	1.25		m,p-Xylene[a]	0.9969	12.5	5%	7.8
	2,3-Dimethyl-pentane	0.9969	6.2	5%	1.34		o-Xylene	0.9954	5.2	4%	7.64
	3-Methyl-hexane	0.9946	8.8	7%	1.61	**Aromatic**	Styrene	0.9961	10.6	8%	1.73
	2,2,4-Trimethyl-pentane	0.9975	7.1	6%	1.26		Isopropylbenzene	0.9947	4.3	4%	2.52
	n-Heptane	0.9974	9	7%	1.07		n-Propylbenzene	0.9929	1.6	1%	2.03
	Methyl-cyclohexane	0.9972	5.8	5%	1.7		m-Ethyltoluene	0.9910	7.3	6%	7.39
	2,3,4-Trimethyl-pentane	0.9976	5.7	5%	1.03		p-Ethyltoluene	0.9994	8.4	7%	4.44

	2-Methyl-heptane	0.9971	7.0	6%	1.07	1,3,5-Trimethyl-benzene	0.9994	6.1	5%	11.76
	3-Methyl-heptane	0.9974	6.7	5%	1.24	o-Ethyltoluene	0.9995	4.3	4%	5.59
	n-Octane	0.9973	7.6	6%	0.9	1,2,4-Trimethylbenzene	0.9983	9.7	8%	8.87
	n-Nonane	0.9963	3.4	3%	0.78	1,2,3-Trimethylbenzene	0.9927	9.7	8%	11.97
	n-Decane	0.9935	7.8	6%	0.68	m-Diethylbenzene	0.9967	5.2	4%	7.1
	n-Undecane	0.9919	7.5	6%	0.61	p-Diethylbenzene	0.9950	4.2	3%	4.43

529 [a] *m*-Xylene and *p*-Xylene are co-eluted in the chromatographic separation.

530

Atmos. Chem. Phys. Discuss., https://doi.org/10.5194/acp-2018-397
Manuscript under review for journal Atmos. Chem. Phys.
Discussion started: 10 August 2018

Atmospheric Chemistry and Physics Discussions

531 Table 2. Wind speed ($m \cdot s^{-1}$) during the sampling period

	JK	MEM	YH	GS
May	1.34±0.65	1.86±1.19	1.27±0.66	0.97±0.49
June	1.07±0.48	1.86±0.94	0.97±0.36	0.74±0.33
July	1.48±0.59	2.62±1.19	1.15±0.45	0.90±0.32
August	1.06±0.48	1.86±0.94	0.95±0.39	0.76±0.35
September	0.80±0.38	1.24±0.80	0.82±0.43	0.62±0.38

532

533

Atmos. Chem. Phys. Discuss., https://doi.org/10.5194/acp-2018-397
Manuscript under review for journal Atmos. Chem. Phys.
Discussion started: 10 August 2018

Atmospheric Chemistry and Physics Discussions

534 Table 3. Concentrations of Top 10 PAMS and Σ_{PAMS} (ppbv) at every site during the sampling
535 period

Site		JK			MEM			GS			YH	
Item	Species	Mean	Std.	Species	Mean	Std.	Species	Mean	Std.	Species	Mean	Std.
	Acetylene	4.39	2.48	Ethane	5.17	2.18	Ethane	4.71	2.18	Acetylene	4.74	2.61
	Ethane	4.29	1.43	Acetylene	4.22	1.60	Propane	3.55	3.79	Ethane	4.42	1.87
	Ethylene	3.77	2.57	Ethylene	3.42	1.70	Acetylene	3.14	1.69	Ethylene	4.27	4.02
	Toluene	3.19	3.36	Propane	3.02	2.05	Toluene	3.05	3.66	Propane	2.58	1.48
	Propane	2.61	1.23	n-Butane	1.77	1.68	Ethylene	2.92	1.92	Toluene	2.28	2.60
May.2017	Isopentane	2.52	3.03	Benzene	1.68	2.48	2-Methylpentane	2.56	6.54	n-Butane	1.54	0.95
	n-Butane	2.20	1.75	Toluene	1.59	1.53	Isopentane	1.97	1.38	Isopentane	1.32	1.04
	m,p-Xylene[a]	2.17	2.63	Isopentane	1.21	0.70	n-Butane	1.78	1.80	Isoprene	1.32	1.31
	Benzene	1.87	2.11	2-Methylpentane	1.13	2.19	Cyclohexane	1.58	4.72	Benzene	1.19	1.07
	Isoprene	1.75	1.67	Isobutane	1.13	1.33	Isobutane	1.52	3.14	Isobutane	0.84	0.53
	Σ_{PAMS}	37.65	22.58	Σ_{PAMS}	29.30	15.34	Σ_{PAMS}	31.73	18.70	Σ_{PAMS}	30.05	16.43
	Acetylene	4.62	1.50	Ethane	6.33	3.09	Acetylene	5.03	1.83	Acetylene	4.60	1.41
	Ethane	3.48	1.47	Cyclohexane	5.18	11.87	Ethane	4.49	2.52	Ethane	3.85	1.46
	Ethylene	3.22	1.52	Isopentane	4.95	8.30	Ethylene	3.27	1.16	Ethylene	3.05	0.90
	Propane	2.32	1.43	Toluene	4.35	8.21	Toluene	3.14	3.03	Propane	2.48	0.99
	n-Butane	2.30	2.98	Isobutane	4.16	10.30	Ethane	3.09	2.07	Isoprene	1.67	1.62
June.2017	Isoprene	2.08	1.58	Propane	3.66	3.66	n-Butane	1.84	1.53	n-Butane	1.54	0.87
	Toluene	1.99	1.79	Acetylene	3.45	2.05	m,p-Xylene[a]	1.83	2.75	Toluene	1.44	1.65
	m,p-Xylene[a]	1.69	2.00	n-Butane	2.51	3.51	Isopentane	1.74	1.58	Isopentane	1.38	1.30
	Isopentane	1.59	1.56	Benzene	2.50	4.58	Isobutane	1.70	2.63	Benzene	1.04	0.61
	Benzene	1.30	0.72	Ethylene	2.41	1.34	Benzene	1.41	0.90	Isobutane	0.99	0.49
	Σ_{PAMS}	34.02	19.89	Σ_{PAMS}	30.28	12.77	Σ_{PAMS}	39.29	25.37	Σ_{PAMS}	28.33	11.94
	Acetylene	2.55	1.47	Ethane	4.00	2.08	Ethane	2.96	1.80	Ethane	2.75	0.77
July.2017	Ethane	2.30	0.95	Isopentane	2.13	3.84	Propane	2.56	2.23	Acetylene	1.84	0.73

Atmos. Chem. Phys. Discuss., https://doi.org/10.5194/acp-2018-397
Manuscript under review for journal Atmos. Chem. Phys.
Discussion started: 10 August 2018

Atmospheric Chemistry and Physics Discussions

	n-Butane	1.46	0.84	Acetylene	2.11	0.86	Isopentane	1.99	2.09	Isopentane	1.73	2.30
	Isoprene	1.42	1.45	Propane	2.08	1. 31	Acetylene	1.58	0.71	Propane	1.52	0.57
	Propane	1.38	0.65	Ethylene	1.36	0.97	Isobutane	1.37	1.85	Trans-2-pentene	1.36	1.49
	Isopentane	1.26	1.24	n-Butane	1.36	1.12	n-Butane	1.36	1.12	n-Butane	1.08	0.55
	Ethylene	1.20	0.84	Isobutane	1.05	1.58	Ethylene	1.18	1.05	Ethylene	1.05	0.65
	Isobutane	0.75	0.57	Toluene	0.72	0.74	Toluene	1.15	1.81	Isobutane	0.98	1.22
	Benzene	0.51	0.22	Benzene	0.55	0.34	Isoprene	1.12	0.99	Toluene	0.62	0.71
	Toluene	0.49	0.45	Isoprene	0.54	0.52	n-Pentane	0.60	0.60	Benzene	0.55	0.36
	Σ_{PAMS}	16.01	6.13	Σ_{PAMS}	20.74	12.66	Σ_{PAMS}	19.60	13.94	Σ_{PAMS}	15.95	7.54
	Ethane	3.41	1.62	Ethane	5.90	2.88	Ethane	3.97	2.51	Ethane	3.77	1.43
	Isopentane	2.69	2.98	Isopentane	3.49	7.25	Acetylene	2.45	2.08	Propane	2.81	1.27
	Propane	2.38	1.72	Propane	2.58	1.40	Propane	2.12	1.33	Isopentane	2.58	3.93
	Acetylene	1.94	1.01	Acetylene	2.19	1.50	Isopentane	1.51	1.41	Acetylene	2.04	1.11
	n-Butane	1.81	1.65	Ethylene	1.43	0.99	Ethylene	1.35	1.09	n-Butane	1.75	0.85
Aug.2017	Ethylene	1.52	1.28	n-Butane	1.41	0.90	Toluene	1.28	1.97	n-Pentane	1.72	2.63
	Isoprene	1.02	0.99	n-Pentane	1.10	1.88	n-Butane	1.25	0.91	Toluene	1.52	1.85
	n-Pentane	0.98	0.89	Toluene	0.98	1.40	Isoprene	0.87	0.77	Ethylene	1.32	0.70
	Isobutane	0.90	0.71	Isobutane	0.91	0.76	n-Pentane	0.76	0.72	Isobutane	1.14	0.82
	Toluene	0.89	0.98	Benzene	0.53	0.28	Isobutane	0.68	0.47	Trans-2-pentene	1.11	1.39
	Σ_{PAMS}	21.54	15.29	Σ_{PAMS}	24.37	20.79	Σ_{PAMS}	20.49	15.67	Σ_{PAMS}	26.03	17.01
	Ethane	4.66	2.21	Ethane	6.87	3.92	Propane	10.77	17.73	Ethane	5.35	2.65
	Propane	3.54	2.19	Acetylene	3.82	3.76	n-Butane	7.55	13.79	Acetylene	5.08	8.36
	Acetylene	3.27	3.09	Isopentane	3.73	6.25	Isobutane	5.46	10.76	Toluene	4.37	5.28
	n-Butane	2.52	1.96	Propane	3.31	1.83	Isopentane	5.25	8.76	Propane	3.29	1.93
Sept.2017	Ethylene	2.02	1.48	Toluene	2.71	4.31	Ethane	5.08	2.20	Isopentane	2.89	3.02
	Isopentane	1.77	1.49	Ethylene	2.37	1.55	Acetylene	4.03	5.84	Ethylene	2.67	2.03
	Toluene	1.44	1.42	n-Butane	2.23	1.53	Toluene	2.50	3.54	n-Butane	2.47	2.19
	Isobutane	1.08	0.79	n-Pentane	1.70	2.63	n-Pentane	2.33	3.44	n-Pentane	1.39	1.22

m,p-Xylene[a]	0.93	1.13	Isobutane	1.33	1.10	Ethylene	2.19	1.68	Isobutane	1.19	0.86
n-Pentane	0.75	0.61	Benzene	0.60	0.43	Propylene	0.73	0.76	m,p-Xylene[a]	1.09	1.62
Σ_{PAMS}	26.20	16.22	Σ_{PAMS}	34.15	23.85	Σ_{PAMS}	30.36	19.76	Σ_{PAMS}	32.56	19.76

536 [a] *m*-Xylene and *p*-Xylene are co-eluted in the chromatographic separation.

537

Atmos. Chem. Phys. Discuss., https://doi.org/10.5194/acp-2018-397
Manuscript under review for journal Atmos. Chem. Phys.
Discussion started: 10 August 2018

Atmospheric Chemistry and Physics Discussions

538

539 Table 4. Average mixing ratios of NO_x, O_3, CO, SO_2 and Σ_{PAMS} in the sampling campaign

Site	NOx	O_3	CO	SO_2	Σ_{PAMS}
GS	32.21±27.24	52.53±36.02	0.84±0.28	6.80±4.33	31.66±28.73
JK	34.11±34.17	49.50±33.66	0.79±0.31	4.51±3.24	28.63±22.04
MEM	36.42±32.21	47.09±32.66	0.92±0.31	6.44±4.75	27.67±18.09
YH	29.31±27.84	52.00±31.92	0.84±0.25	4.95±3.88	27.45±18.28

540 Note: Units for air pollutants were ppbv except for CO, which was measured in ppmv

541

Atmos. Chem. Phys. Discuss., https://doi.org/10.5194/acp-2018-397
Manuscript under review for journal Atmos. Chem. Phys.
Discussion started: 10 August 2018

Atmospheric Chemistry and Physics Discussions

542 Table 5. Top 10 PAMS ranked according to calculated ozone formation potential (OFP)

JK			MEM			YH			GS		
species	OFP(ppbv)	(%)	species	OFP(ppbv)	(%)	species	OFP(ppbv)	(%)	species	OFP(ppbv)	(%)
Ethylene	18.99	25.54	Ethylene	18.44	30.88	Ethylene	19.83	28.10	Ethylene	18.04	25.96
Isoprene	12.99	21.83	Isoprene	4.66	10.10	Isoprene	7.44	11.30	Isoprene	8.01	16.75
m/p-Xylene[a]	6.08	5.89	Toluene	3.73	6.67	Toluene	6.63	7.75	Toluene	7.43	7.67
Toluene	5.53	5.83	Propylene	3.60	6.16	m/p-Xylene[a]	3.93	4.38	Propylene	4.39	5.85
Propylene	4.03	5.36	Acetylene	2.82	5.00	Acetylene	3.15	4.38	m/p-Xylene[a]	4.31	4.57
Acetylene	2.97	4.44	m/p-Xylene[a]	2.55	4.20	Propylene	3.01	3.60	Acetylene	2.76	4.24
n-Butane	2.15	3.05	n-Butane	1.81	3.20	Trans-2-pentene	2.25	2.94	n-Butane	1.82	2.93
o-Xylene	1.83	2.00	Isopentane	1.76	3.16	n-Butane	1.84	2.80	Isopentane	1.71	2.68
Isopentane	1.66	1.95	Ethane	1.58	2.96	Isopentane	1.59	2.22	Propane	1.38	2.26
Propane	1.17	1.73	Propane	1.31	2.48	Propane	1.18	1.98	Isobutane	1.13	1.98

543 [a] *m*-Xylene and *p*-Xylene are co-eluted in the chromatographic separation.

544

545

Atmos. Chem. Phys. Discuss., https://doi.org/10.5194/acp-2018-397
Manuscript under review for journal Atmos. Chem. Phys.
Discussion started: 10 August 2018

Atmospheric Chemistry and Physics Discussions

546 Table 6. Critical parameters for optimizing the PMF results

Site	JK			MEM			YH			GS		
Factor Number	**6**	**7**	**8**	**5**	**6**	**7**	**6**	**7**	**8**	**6**	**7**	**8**
Q(true)	2821.61	2246.40	1859.77	2793.06	2207.56	1789.63	2903.47	2458.26	2025.64	3396.21	2897.95	2520.45
Q(robust)	2840.41	2263.57	1877.59	2808.12	2229.95	1793.15	2925.13	2469.35	2033.93	3426.53	2919.45	2539.44
Q(true)/Q(exp)	1.16	**0.98**	0.86	1.13	**0.94**	0.80	1.17	**1.04**	0.91	1.45	1.30	**1.20**

547

548

Atmos. Chem. Phys. Discuss., https://doi.org/10.5194/acp-2018-397
Manuscript under review for journal Atmos. Chem. Phys.
Discussion started: 10 August 2018

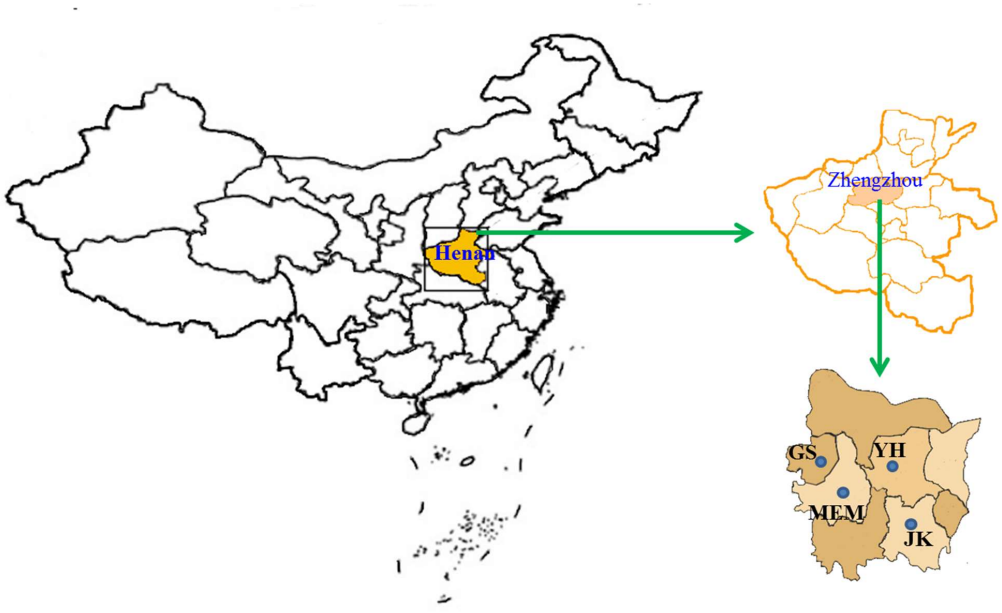

549

550 Fig 1. Map of Zhengzhou, China showing the locations of sampling sites.

551

Atmos. Chem. Phys. Discuss., https://doi.org/10.5194/acp-2018-397
Manuscript under review for journal Atmos. Chem. Phys.
Discussion started: 10 August 2018

552

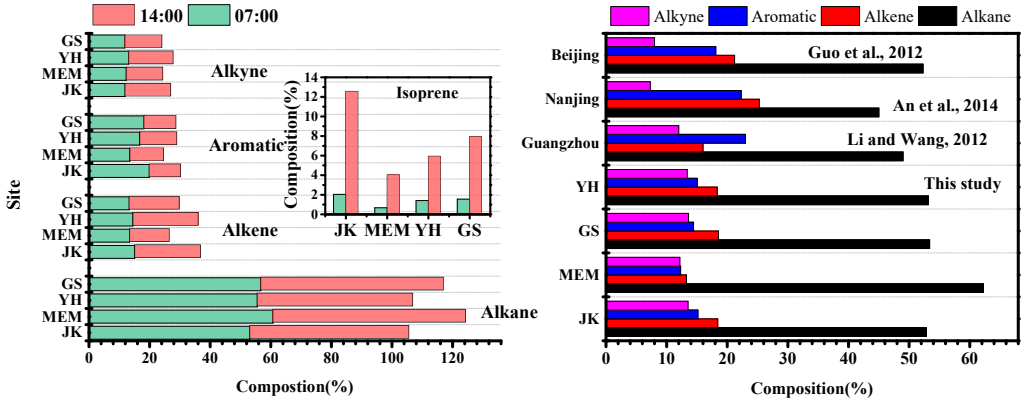

Fig 2. Compositions of major organic classes and comparison between Zhengzhou and other cities in China

Atmos. Chem. Phys. Discuss., https://doi.org/10.5194/acp-2018-397
Manuscript under review for journal Atmos. Chem. Phys.
Discussion started: 10 August 2018

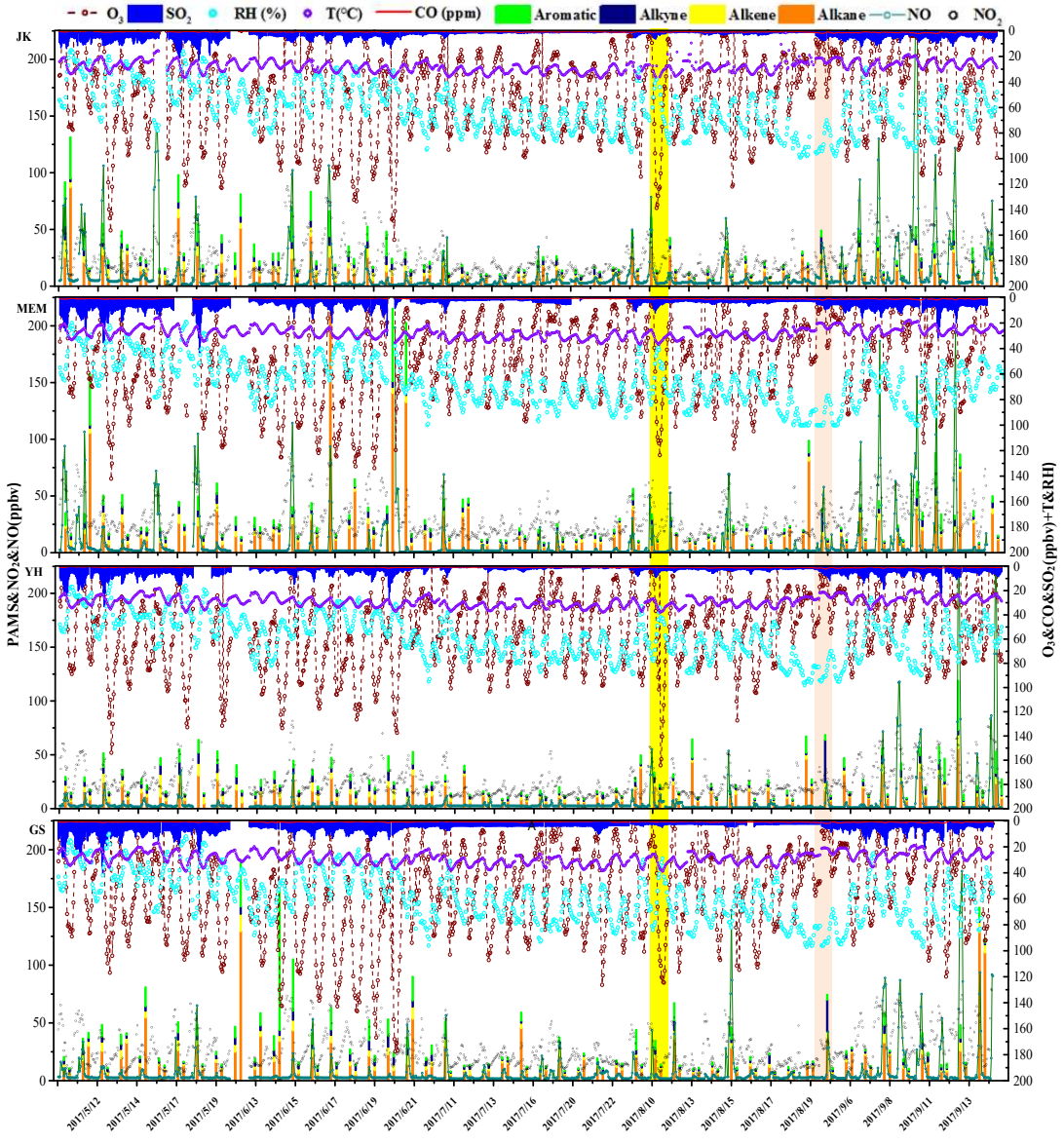

Fig 3. Temporal variations of mixing ratios of PAMS, CO, SO_2, NO, NO_2 and O_3 and meteorological conditions at each site. 10th of August and 5th of September are highlighted as yellow and pink, respectively.

Atmos. Chem. Phys. Discuss., https://doi.org/10.5194/acp-2018-397
Manuscript under review for journal Atmos. Chem. Phys.
Discussion started: 10 August 2018

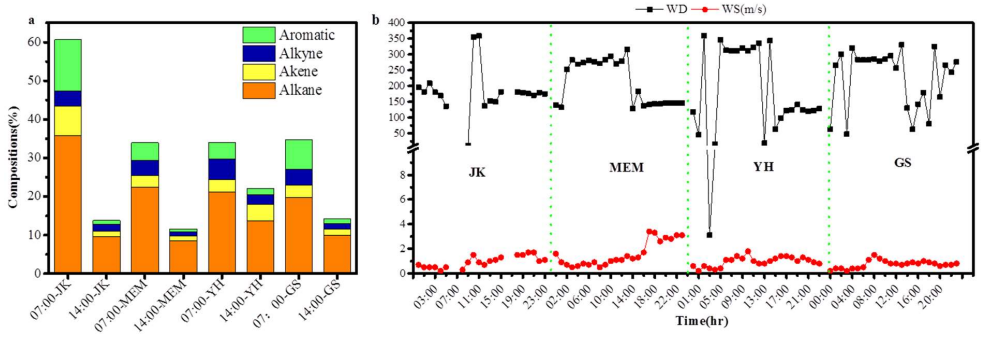

559

560 Fig.4. Temporal variation of compositions, wind direction and wind speed on 10th of August 2017

561

562

563

564

Atmos. Chem. Phys. Discuss., https://doi.org/10.5194/acp-2018-397
Manuscript under review for journal Atmos. Chem. Phys.
Discussion started: 10 August 2018

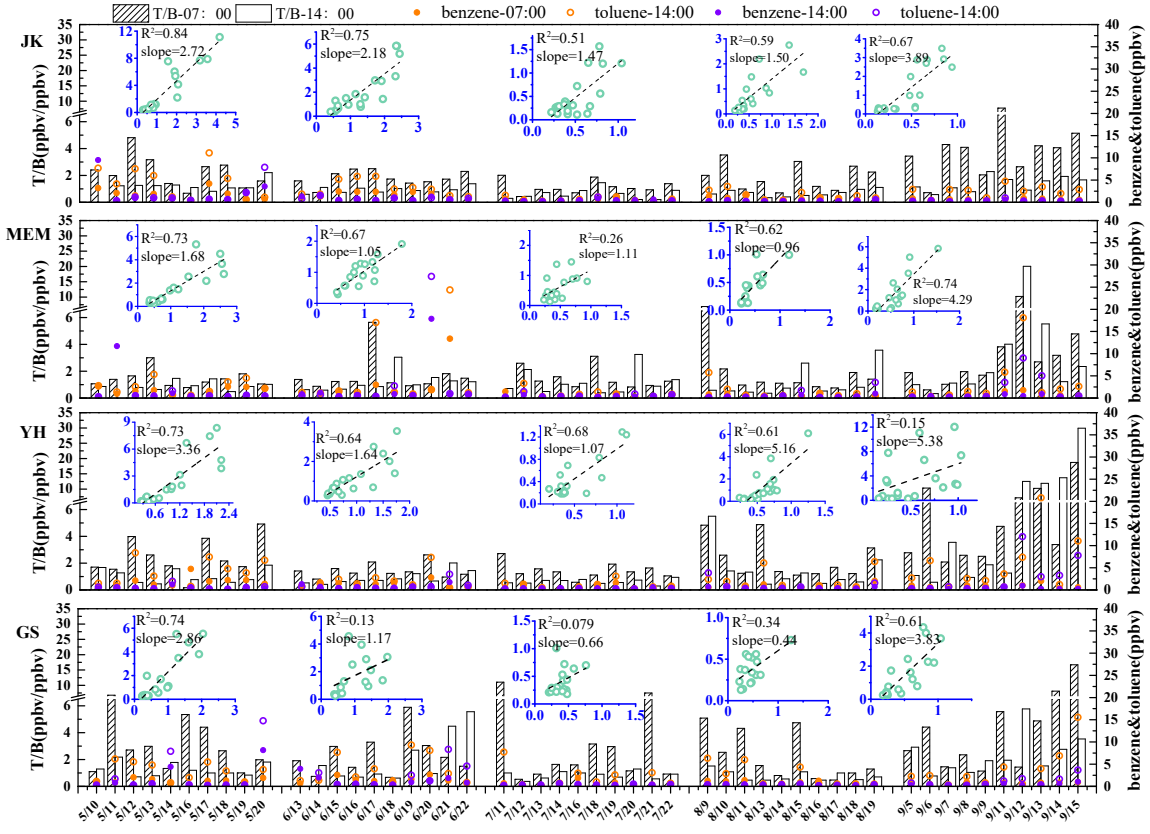

Fig 5. Time series of benzene and toluene and the correlation analysis between these two compounds at every site

Note: The vertical axis in every small figure represents the mixing ratio of toluene (ppbv), while the horizontal axis stands for benzene level (ppbv).

Atmos. Chem. Phys. Discuss., https://doi.org/10.5194/acp-2018-397
Manuscript under review for journal Atmos. Chem. Phys.
Discussion started: 10 August 2018

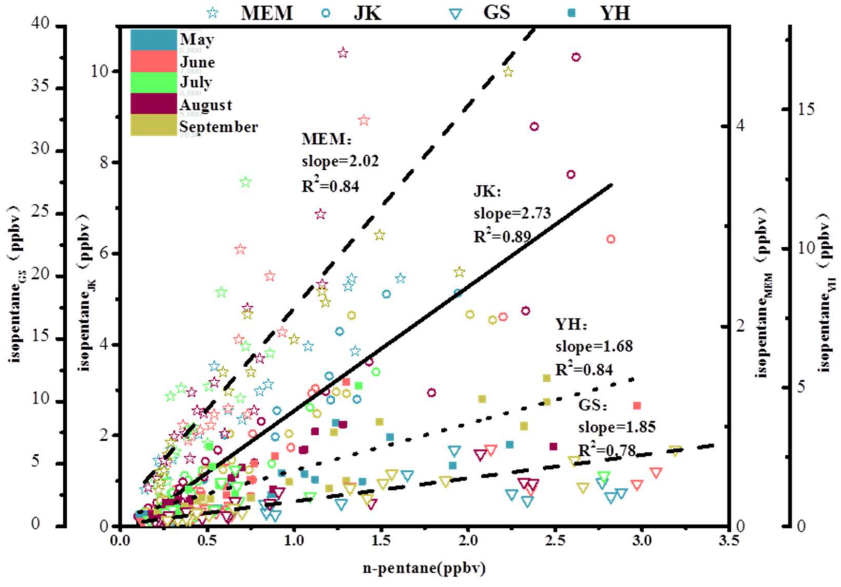

572

573 Fig 6. Ratios of isopentane to n-pentane at every site

574

Atmos. Chem. Phys. Discuss., https://doi.org/10.5194/acp-2018-397
Manuscript under review for journal Atmos. Chem. Phys.
Discussion started: 10 August 2018

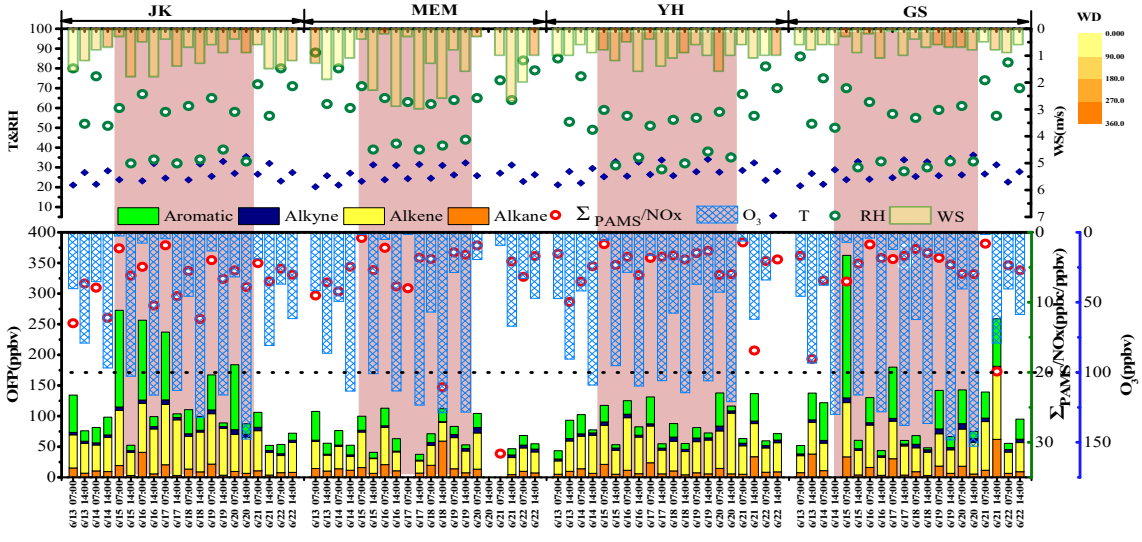

Fig 7. Spatio-temporal variations in meteorological factors, OFP of each organic group, Σ_{PAMS}/NO_x, and mixing ratios of O_3 in June. Clear days at RH<45% are highlighted in pink.

Atmos. Chem. Phys. Discuss., https://doi.org/10.5194/acp-2018-397
Manuscript under review for journal Atmos. Chem. Phys.
Discussion started: 10 August 2018

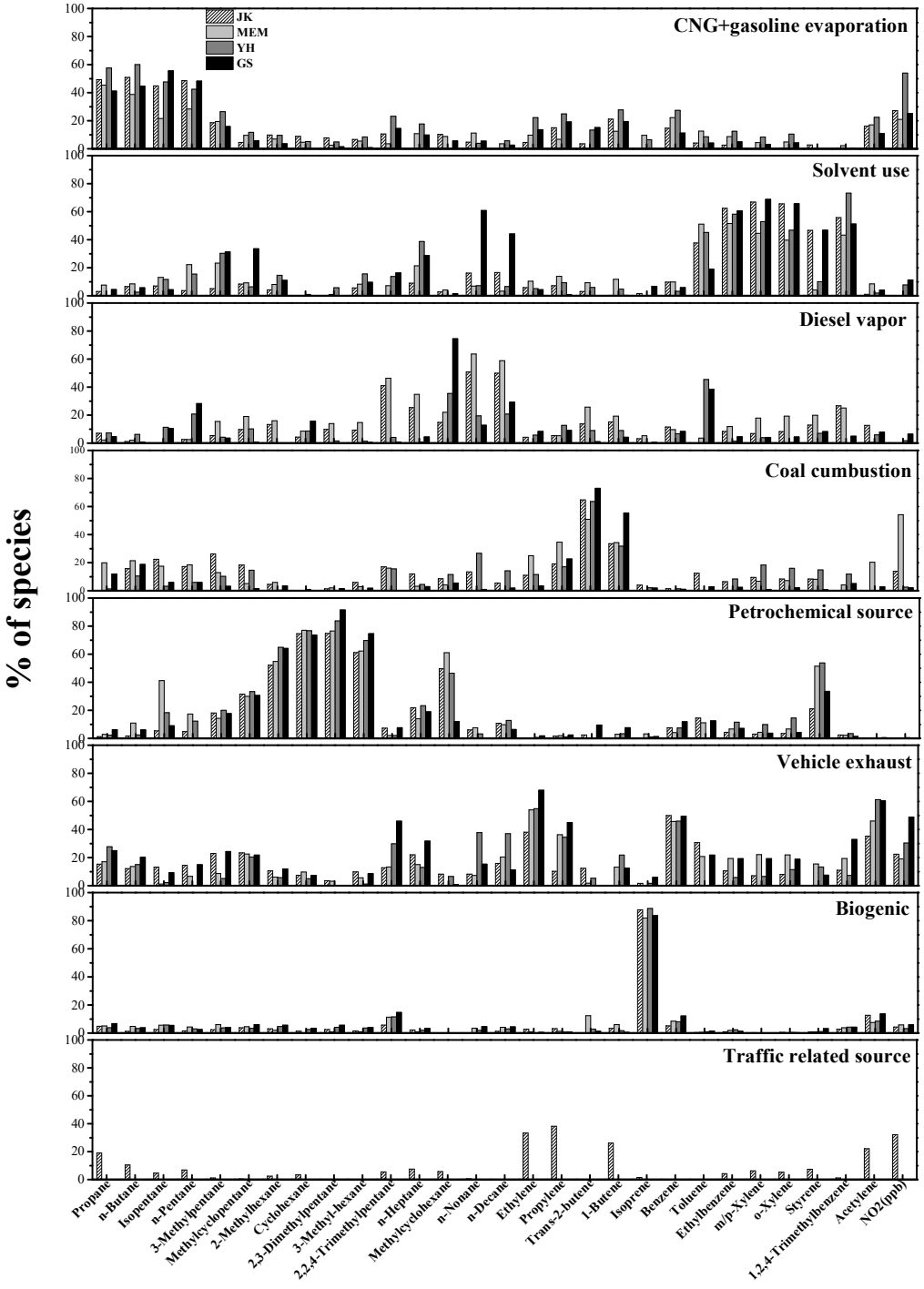

587

Atmos. Chem. Phys. Discuss., https://doi.org/10.5194/acp-2018-397
Manuscript under review for journal Atmos. Chem. Phys.
Discussion started: 10 August 2018

588 Fig. 8 Explained variations in source profiles as identified by PMF

589

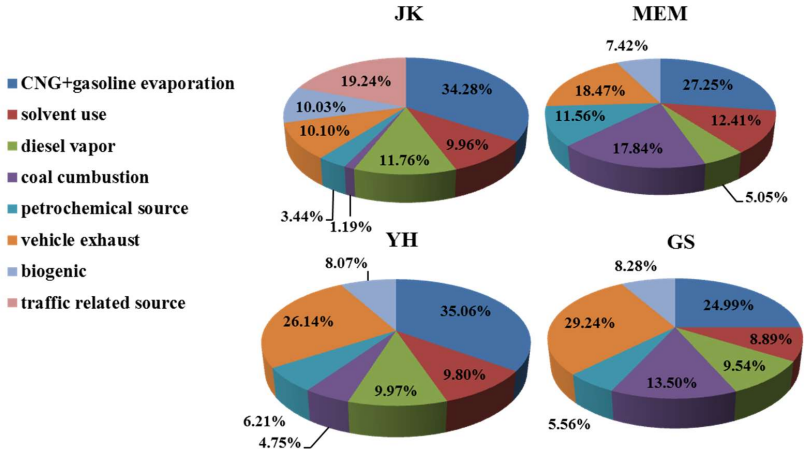

590

591 Fig 9. Source apportionment results during the whole sampling period.

592

Atmos. Chem. Phys. Discuss., https://doi.org/10.5194/acp-2018-397
Manuscript under review for journal Atmos. Chem. Phys.
Discussion started: 10 August 2018

593

May

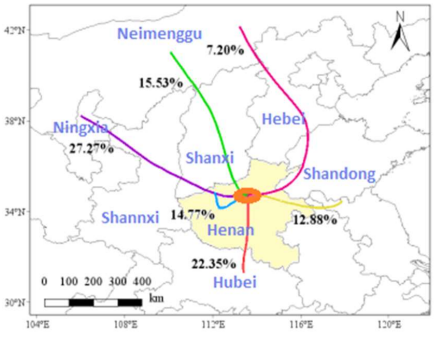

June

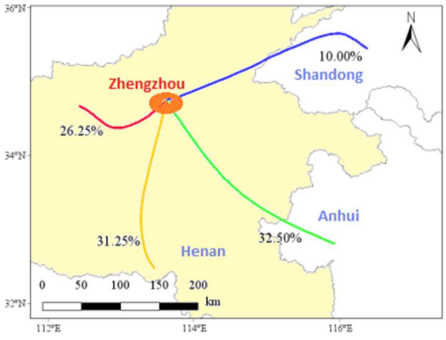

July

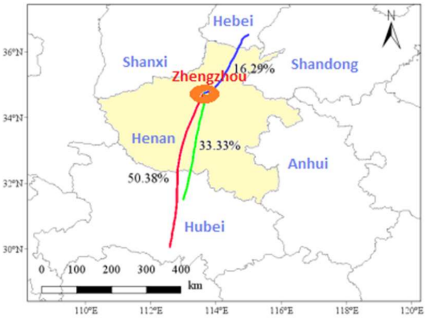

August

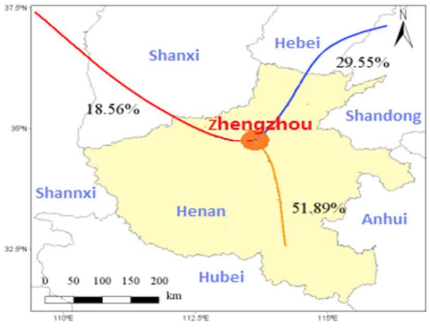

September

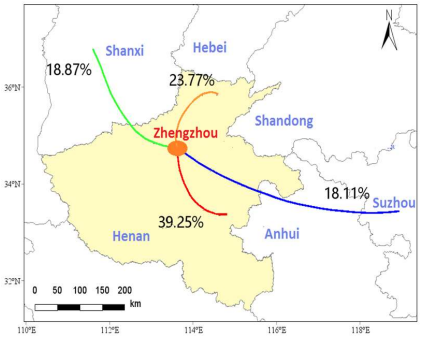

594 Fig 10. Cluster analysis of Zhengzhou in each sampling month

595

596 **Ref.**

597 Abeleira, A., Pollack, I. B., Sive, B., Zhou, Y., Fischer, E. V., and Farmer, D. K.: Source characterization of volatile
598 organic compounds in the Colorado Northern Front Range Metropolitan Area during spring and summer 2015, Journal
599 of Geophysical Research: Atmospheres, 10.1002/2016jd026227, 2017.
600 Akagi, S. K., Yokelson, R. J., Wiedinmyer, C., Alvarado, M. J., Reid, J. S., Karl, T., Crounse, J. D., and Wennberg, P.
601 O.: Emission factors for open and domestic biomass burning for use in atmospheric models, Atmospheric Chemistry
602 and Physics, 11, 4039-4072, 10.5194/acp-11-4039-2011, 2011.
603 An, J., Zhu, B., Wang, H., Li, Y., Lin, X., and Yang, H.: Characteristics and source apportionment of VOCs measured
604 in an industrial area of Nanjing, Yangtze River Delta, China, Atmospheric Environment, 97, 206-214,
605 10.1016/j.atmosenv.2014.08.021, 2014.
606 Barletta, B., Meinardi, S., Sherwood Rowland, F., Chan, C.-Y., Wang, X., Zou, S., Yin Chan, L., and Blake, D. R.:
607 Volatile organic compounds in 43 Chinese cities, Atmospheric Environment, 39, 5979-5990,
608 10.1016/j.atmosenv.2005.06.029, 2005.
609 Blanchard, C. L., and Hidy, G. M.: Ozone Response to Emission Reductions in the Southeastern United States,
610 Atmospheric Chemistry and Physics Discussions, 1-33, 10.5194/acp-2017-534, 2017.
611 Capps, S. L., Hu, Y., and Russell, A. G.: Assessing Near-Field and Downwind Impacts of Reactivity-Based
612 Substitutions, Journal of the Air & Waste Management Association, 60, 316-327, 10.3155/1047-3289.60.3.316, 2012.
613 Carter, W.P.L.: Updated maximum incremental reactivity scale and hydrocarbon bin reactivities for regulatory
614 applications, Prepared for California Air Resources Board Contract 07-339, 2010.
615 Chen, S.-P., Liu, T.-H., Chen, T.-F., Yang, C.-F. O., Wang, J.-L., and Chang, J. S.: Diagnostic Modeling of PAMS
616 VOC Observation, Environ. Sci. Technol., 44, 4635–4644, 2010.
617 Chen, W. T., Shao, M., Lu, S. H., Wang, M., Zeng, L. M., Yuan, B., and Liu, Y.: Understanding primary and secondary
618 sources of ambient carbonyl compounds in Beijing using the PMF model, Atmospheric Chemistry and Physics, 14,
619 3047-3062, 10.5194/acp-14-3047-2014, 2014.
620 Cheng, L., Fu, L., Angle, R. P., and Sandhu, H. S.: Seasonal variations of volatile organic compounds in Edmonton,
621 Alberta, Atmospheric Environment, 31, 239-246, 1997.
622 Duan, J., Tan, J., Yang, L., Wu, S., and Hao, J.: Concentration, sources and ozone formation potential of volatile
623 organic compounds (VOCs) during ozone episode in Beijing, Atmospheric Research, 88, 25-35,
624 10.1016/j.atmosres.2007.09.004, 2008.
625 Gao, W., Tie, X., Xu, J., Huang, R., Mao, X., Zhou, G., and Chang, L.: Long-term trend of O3 in a mega City
626 (Shanghai), China: Characteristics, causes, and interactions with precursors, The Science of the total environment,
627 603-604, 425-433, 10.1016/j.scitotenv.2017.06.099, 2017.
628 Geddes, J. A., Murphy, J. G., and Wang, D. K.: Long term changes in nitrogen oxides and volatile organic compounds
629 in Toronto and the challenges facing local ozone control, Atmospheric Environment, 43, 3407-3415,
630 10.1016/j.atmosenv.2009.03.053, 2009.
631 Geng, F., Zhang, Q., Tie, X., Huang, M., Ma, X., Deng, Z., Yu, Q., Quan, J., and Zhao, C.: Aircraft measurements of
632 O3, NOx, CO, VOCs, and SO2 in the Yangtze River Delta region, Atmospheric Environment, 43, 584-593,
633 10.1016/j.atmosenv.2008.10.021, 2009.
634 Geng, N., Wang, J., Xu, Y., Zhang, W., Chen, C., and Zhang, R.: PM2.5 in an industrial district of Zhengzhou, China:
635 Chemical composition and source apportionment, Particuology, 11, 99-109, 10.1016/j.partic.2012.08.004, 2013.

636 Gentner, D. R., Worton, D. R., Isaacman, G., Davis, L. C., Dallmann, T. R., Wood, E. C., Herndon, S. C., Goldstein, A.
637 H., and Harley, R. A.: Chemical composition of gas-phase organic carbon emissions from motor vehicles and
638 implications for ozone production, Environmental science & technology, 47, 11837-11848, 10.1021/es401470e, 2013.
639 Gilman, J. B., Lerner, B. M., Kuster, W. C., and de Gouw, J. A.: Source signature of volatile organic compounds from
640 oil and natural gas operations in northeastern Colorado, Environmental science & technology, 47, 1297-1305,
641 10.1021/es304119a, 2013.
642 Gong, M., Yin, S., Gu, X., Xu, Y., Jiang, N., and Zhang, R.: Refined 2013-based vehicle emission inventory and its
643 spatial and temporal characteristics in Zhengzhou, China, The Science of the total environment, 599-600, 1149-1159,
644 10.1016/j.scitotenv.2017.03.299, 2017.
645 Guo, H., Cheng, H. R., Ling, Z. H., Louie, P. K., and Ayoko, G. A.: Which emission sources are responsible for the
646 volatile organic compounds in the atmosphere of Pearl River Delta?, Journal of hazardous materials, 188, 116-124,
647 10.1016/j.jhazmat.2011.01.081, 2011.
648 Guo, H., Ling, Z. H., Cheng, H. R., Simpson, I. J., Lyu, X. P., Wang, X. M., Shao, M., Lu, H. X., Ayoko, G., Zhang, Y.
649 L., Saunders, S. M., Lam, S. H. M., Wang, J. L., and Blake, D. R.: Tropospheric volatile organic compounds in China,
650 The Science of the total environment, 574, 1021-1043, 10.1016/j.scitotenv.2016.09.116, 2017.
651 Guo, S., Tan, J., Duan, J., Ma, Y., Yang, F., He, K., and Hao, J.: Characteristics of atmospheric non-methane
652 hydrocarbons during haze episode in Beijing, China, Environmental monitoring and assessment, 184, 7235-7246,
653 10.1007/s10661-011-2493-9, 2012.
654 Han, D., Gao, S., Fu, Q., Cheng, J., Chen, X., Xu, H., Liang, S., Zhou, Y., and Ma, Y.: Do volatile organic compounds
655 (VOCs) emitted from petrochemical industries affect regional PM 2.5 ?, Atmospheric Research, 209, 123-130,
656 10.1016/j.atmosres.2018.04.002, 2018.
657 Hidy, G. M., and Blanchard, C. L.: Precursor reductions and ground-level ozone in the Continental United States,
658 Journal of the Air & Waste Management Association, 65, 1261-1282, 10.1080/10962247.2015.1079564, 2015.
659 Ho, K. F., Lee, S. C., Ho, W. K., Blake, D. R., Cheng, Y., Li, Y. S., Ho, S. S. H., Fung, K., Louie, P. K. K., and Park,
660 D.: Vehicular emission of volatile organic compounds (VOCs) from a tunnel study in Hong Kong, Atmos. Chem. Phys.,
661 9, 7491–7504, 2009.
662 Hoque, R. R., Khillare, P. S., Agarwal, T., Shridhar, V., and Balachandran, S.: Spatial and temporal variation of BTEX
663 in the urban atmosphere of Delhi, India, The Science of the total environment, 392, 30-40,
664 10.1016/j.scitotenv.2007.08.036, 2008.
665 Huang, C., Wang, H. L., Li, L., Wang, Q., Lu, Q., de Gouw, J. A., Zhou, M., Jing, S. A., Lu, J., and Chen, C. H.: VOC
666 species and emission inventory from vehicles and their SOA formation potentials estimation in Shanghai, China,
667 Atmospheric Chemistry and Physics, 15, 11081-11096, 10.5194/acp-15-11081-2015, 2015a.
668 Huang, X., Zhang, Y., Yang, W., Huang, Z., Wang, Y., Zhang, Z., He, Q., Lü, S., Huang, Z., Bi, X., and Wang, X.:
669 Effect of traffic restriction on reducing ambient volatile organic compounds (VOCs): Observation-based evaluation
670 during a traffic restriction drill in Guangzhou, China, Atmospheric Environment, 161, 61-70,
671 10.1016/j.atmosenv.2017.04.035, 2017.
672 Huang, Y., Ling, Z. H., Lee, S. C., Ho, S. S. H., Cao, J. J., Blake, D. R., Cheng, Y., Lai, S. C., Ho, K. F., Gao, Y., Cui,
673 L., and Louie, P. K. K.: Characterization of volatile organic compounds at a roadside environment in Hong Kong: An
674 investigation of influences after air pollution control strategies, Atmospheric Environment, 122, 809-818,
675 10.1016/j.atmosenv.2015.09.036, 2015b.
676 Iannuzzi, A., Verga, M. C., Renis, M., Schiavo, A., Salvatore, V., Santoriello, C., Pazzano, D., Licenziati, M. R., and
677 Polverino, M.: Air pollution and carotid arterial stiffness in children, Cardiology in the young, 20, 186-190,
678 10.1017/S1047951109992010, 2010.

679 IARC: IARC (International Agency for Research on Cancer) Monographs on the Evaluation of Carcinogenic Risks to
680 Human. http://monographs.iarc.fr/ENG/Classification/latest_classif.php. (Accessed on 13 December 2017)
681 Jia, C., Mao, X., Huang, T., Liang, X., Wang, Y., Shen, Y., Jiang, W., Wang, H., Bai, Z., Ma, M., Yu, Z., Ma, J., and
682 Gao, H.: Non-methane hydrocarbons (NMHCs) and their contribution to ozone formation potential in a petrochemical
683 industrialized city, Northwest China, Atmospheric Research, 169, 225-236, 10.1016/j.atmosres.2015.10.006, 2016.
684 Jin, X., and Holloway, T.: Spatial and temporal variability of ozone sensitivity over China observed from the Ozone
685 Monitoring Instrument, Journal of Geophysical Research: Atmospheres, 120, 7229-7246, 10.1002/2015jd023250, 2015.
686 Jobson, B. T., Parrish, D. D., Goldan, P., Kuster, W., Fehsenfeld, F. C., Blake, D. R., Blake, N. J., and Niki, H.: Spatial
687 and temporal variability of nonmethane hydrocarbon mixing ratios and their relation to photochemical lifetime, Journal
688 of Geophysical Research: Atmospheres, 103, 13557-13567, 10.1029/97jd01715, 1998.
689 Jobson, B. T., Berkowitz, C. M., Kuster, W. C., Goldan, P. D., Williams, E. J., Fesenfeld, F. C., Apel, E. C., Karl, T.,
690 Lonneman, W. A., and Riemer, D.: Hydrocarbon source signatures in Houston, Texas: Influence of the petrochemical
691 industry, Journal of Geophysical Research, 109, 10.1029/2004jd004887, 2004.
692 Langford, A. O., Senff, C. J., Alvarez, R. J., Banta, R. M., and Hardesty, R. M.: Long-range transport of ozone from the
693 Los Angeles Basin: A case study, Geophysical Research Letters, 37, n/a-n/a, 10.1029/2010gl042507, 2010.
694 Lau, A. K., Yuan, Z., Yu, J. Z., and Louie, P. K.: Source apportionment of ambient volatile organic compounds in
695 Hong Kong, The Science of the total environment, 408, 4138-4149, 10.1016/j.scitotenv.2010.05.025, 2010.
696 Li, B., Ho, S. S. H., Xue, Y., Huang, Y., Wang, L., Cheng, Y., Dai, W., Zhong, H., Cao, J., and Lee, S.:
697 Characterizations of volatile organic compounds (VOCs) from vehicular emissions at roadside environment: The first
698 comprehensive study in Northwestern China, Atmospheric Environment, 161, 1-12, 10.1016/j.atmosenv.2017.04.029,
699 2017a.
700 Li, K., Chen, L., Ying, F., White, S. J., Jang, C., Wu, X., Gao, X., Hong, S., Shen, J., Azzi, M., and Cen, K.:
701 Meteorological and chemical impacts on ozone formation: A case study in Hangzhou, China, Atmospheric Research,
702 10.1016/j.atmosres.2017.06.003, 2017b.
703 Li, K., Li, J., Wang, W., Tong, S., Liggio, J., and Ge, M.: Evaluating the effectiveness of joint emission control policies
704 on the reduction of ambient VOCs: Implications from observation during the 2014 APEC summit in suburban Beijing,
705 Atmospheric Environment, 164, 117-127, 10.1016/j.atmosenv.2017.05.050, 2017c.
706 Li, L., and Wang, X.: Seasonal and diurnal variations of atmospheric non-methane hydrocarbons in Guangzhou, China,
707 International journal of environmental research and public health, 9, 1859-1873, 10.3390/ijerph9051859, 2012.
708 Li, L., Chen, Y., Zeng, L., Shao, M., Xie, S., Chen, W., Lu, S., Wu, Y., and Cao, W.: Biomass burning contribution to
709 ambient volatile organic compounds (VOCs) in the Chengdu–Chongqing Region (CCR), China, Atmospheric
710 Environment, 99, 403-410, 10.1016/j.atmosenv.2014.09.067, 2014.
711 Li, Q., Zhang, L., Wang, T., Wang, Z., Fu, X., and Zhang, Q.: "New" Reactive Nitrogen Chemistry Reshapes the
712 Relationship of Ozone to Its Precursors, Environmental science & technology, 52, 2810-2818, 10.1021/acs.est.7b05771,
713 2018.
714 Lin, X., Traner, M., and Liu, S. C.: On the Nonlinearity of the Tropospheric Ozone Production, Journal Of Geophysical
715 Research, 93, 15879-15888, 1998.
716 Liu, B., Liang, D., Yang, J., Dai, Q., Bi, X., Feng, Y., Yuan, J., Xiao, Z., Zhang, Y., and Xu, H.: Characterization and
717 source apportionment of volatile organic compounds based on 1-year of observational data in Tianjin, China,
718 Environmental pollution, 218, 757-769, 10.1016/j.envpol.2016.07.072, 2016a.
719 Liu, C., Zhang, C., Mu, Y., Liu, J., and Zhang, Y.: Emission of volatile organic compounds fromdomestic coal stove
720 with the actual alternation of flaming and smoldering combustion processes, Environmental Pollution,
721 10.1016/j.envpol.2016.11.089, 2016b.

722 Liu, C., Ma, Z., Mu, Y., Liu, J., Zhang, C., Zhang, Y., Liu, P., and Zhang, H.: The levels, variation characteristics, and
723 sources of atmospheric non-methane hydrocarbon compounds during wintertime in Beijing, China, Atmospheric
724 Chemistry and Physics, 17, 10633-10649, 10.5194/acp-17-10633-2017, 2017.
725 Liu, H., Liu, S., Xue, B., Lv, Z., Meng, Z., Yang, X., Xue, T., Yu, Q., and He, K.: Ground-level ozone pollution and its
726 health impacts in China, Atmospheric Environment, 173, 223-230, 10.1016/j.atmosenv.2017.11.014, 2018.
727 Liu, Y., Shao, M., Fu, L., Lu, S., Zeng, L., and Tang, D.: Source profiles of volatile organic compounds (VOCs)
728 measured in China: Part I, Atmospheric Environment, 42, 6247-6260, 10.1016/j.atmosenv.2008.01.070, 2008a.
729 Liu, Y., Shao, M., Lu, S., Chang, C.-C., Wang, J.-L., and Fu, L.: Source apportionment of ambient volatile organic
730 compounds in the Pearl River Delta, China: Part II, Atmospheric Environment, 42, 6261-6274,
731 10.1016/j.atmosenv.2008.02.027, 2008b.
732 Liu, Y., Yuan, B., Li, X., Shao, M., Lu, S., Li, Y., Chang, C. C., Wang, Z., Hu, W., Huang, X., He, L., Zeng, L., Hu, M.,
733 and Zhu, T.: Impact of pollution controls in Beijing on atmospheric oxygenated volatile organic compounds (OVOCs)
734 during the 2008 Olympic Games: observation and modeling implications, Atmospheric Chemistry and Physics, 15,
735 3045-3062, 10.5194/acp-15-3045-2015, 2015.
736 Louie, P. K. K., Ho, J. W. K., Tsang, R. C. W., Blake, D. R., Lau, A. K. H., Yu, J. Z., Yuan, Z., Wang, X., Shao, M.,
737 and Zhong, L.: VOCs and OVOCs distribution and control policy implications in Pearl River Delta region, China,
738 Atmospheric Environment, 76, 125-135, 10.1016/j.atmosenv.2012.08.058, 2013.
739 Luecken, D. J., Napelenok, S. L., Strum, M., Scheffe, R., and Phillips, S.: Sensitivity of Ambient Atmospheric
740 Formaldehyde and Ozone to Precursor Species and Source Types Across the United States, Environmental science &
741 technology, 52, 4668-4675, 10.1021/acs.est.7b05509, 2018.
742 Lyu, X. P., Chen, N., Guo, H., Zhang, W. H., Wang, N., Wang, Y., and Liu, M.: Ambient volatile organic compounds
743 and their effect on ozone production in Wuhan, central China, The Science of the total environment, 541, 200-209,
744 10.1016/j.scitotenv.2015.09.093, 2016.
745 Malley, C. S., Braban, C. F., Dumitrean, P., Cape, J. N., and Heal, M. R.: The impact of speciated VOCs on regional
746 ozone increment derived from measurements at the UK EMEP supersites between 1999 and 2012, Atmospheric
747 Chemistry and Physics, 15, 8361-8380, 10.5194/acp-15-8361-2015, 2015.
748 McGaughey, G. R., Desai, N. R., Allen, D. T., Seila, R. L., Lonneman, W. A., Fraser, M. P., Harley, R. A., Pollack, A.
749 K., Ivy, J. M., and Price, J. H.: Analysis of motor vehicle emissions in a Houston tunnel during the Texas Air Quality
750 Study 2000, Atmospheric Environment, 38, 3363-3372, 10.1016/j.atmosenv.2004.03.006, 2004.
751 Millet, D. B., Baasandorj, M., Hu, L., Mitroo, D., Turner, J., and Williams, B. J.: Nighttime Chemistry and Morning
752 Isoprene Can Drive Urban Ozone Downwind of a Major Deciduous Forest, Environmental science & technology, 50,
753 4335-4342, 10.1021/acs.est.5b06367, 2016.
754 Monod, A., Sive, B. C., Avino, P., Chen, T., Blake, D. R., and Rowland, F. S.: Monoaromatic compounds in ambient
755 air of various cities: a focus on correlations between the xylenes and ethylbenzene, Atmospheric Environment, 35,
756 135-149, 2001.
757 Na, K., Kim, Y. P., Moon, K.-C., Moon, I., and Fung, K.: Concentrations of volatile organic compounds in an industrial
758 area of Korea, Atmospheric Environment 35, 2747-2756, 2001.
759 Nagashima, T., Sudo, K., Akimoto, H., Kurokawa, J., and Ohara, T.: Long-term change in the source contribution to
760 surface ozone over Japan, Atmospheric Chemistry and Physics, 17, 8231-8246, 10.5194/acp-17-8231-2017, 2017.
761 Ou, J., Zheng, J., Li, R., Huang, X., Zhong, Z., Zhong, L., and Lin, H.: Speciated OVOC and VOC emission inventories
762 and their implications for reactivity-based ozone control strategy in the Pearl River Delta region, China, The Science of
763 the total environment, 530-531, 393-402, 10.1016/j.scitotenv.2015.05.062, 2015.

764 Ou, J., Yuan, Z., Zheng, J., Huang, Z., Shao, M., Li, Z., Huang, X., Guo, H., and Louie, P. K.: Ambient Ozone Control
765 in a Photochemically Active Region: Short-Term Despiking or Long-Term Attainment?, Environmental science &
766 technology, 50, 5720-5728, 10.1021/acs.est.6b00345, 2016.
767 Paatero, P., and Tapper, U.: Positive matrix factorization: a non-negative Factor model with optimal utilization of Error
768 estimates of data values, Environmetrics, 5, 111-126, 1994.
769 Paatero, P.: Least squares formulation of robust non-negative factor analysis, Chemometrics and Intelligent Laboratory
770 Systems, 37, 23–35, 1997.
771 Paatero, P.: User's Guide for positive Matrix Factorization programs PMF2 and PMF3, part 1-2: Tutorial, 19 -21.
772 University of Helsinki, Helsinki, Finland, 2007.
773 Pal, S., Xueref-Remy, I., Ammoura, L., Chazette, P., Gibert, F., Royer, P., Dieudonné, E., Dupont, J. C., Haeffelin, M.,
774 Lac, C., Lopez, M., Morille, Y., and Ravetta, F.: Spatio-temporal variability of the atmospheric boundary layer depth
775 over the Paris agglomeration: An assessment of the impact of the urban heat island intensity, Atmospheric Environment,
776 63, 261-275, 10.1016/j.atmosenv.2012.09.046, 2012.
777 Polissar, A. V., Hopke, P. K., Paatero, P., Malm, W. C., and Sisler, J. F.: Atmospheric aerosol over Alaska: 2.
778 Elemental composition and sources, Journal of Geophysical Research: Atmospheres, 103, 19045-19057,
779 10.1029/98jd01212, 1998.
780 Pollack, I. B., Ryerson, T. B., Trainer, M., Neuman, J. A., Roberts, J. M., and Parrish, D. D.: Trends in ozone, its
781 precursors, and related secondary oxidation products in Los Angeles, California: A synthesis of measurements from
782 1960 to 2010, Journal of Geophysical Research: Atmospheres, 118, 5893-5911, 10.1002/jgrd.50472, 2013.
783 Raysoni, A. U., Stock, T. H., Sarnat, J. A., Chavez, M. C., Sarnat, S. E., Montoya, T., Holguin, F., and Li, W. W.:
784 Evaluation of VOC concentrations in indoor and outdoor microenvironments at near-road schools, Environmental
785 pollution, 231, 681-693, 10.1016/j.envpol.2017.08.065, 2017.
786 Russo, R. S., Zhou, Y., White, M. L., Mao, H., Talbot, R., and Sive, B. C.: Multi-year (2004–2008) record of
787 nonmethane hydrocarbons and halocarbons in New England: seasonal variations and regional sources, Atmospheric
788 Chemistry and Physics, 10, 4909-4929, 10.5194/acp-10-4909-2010, 2010.
789 Sahu, L. K., Tripathi, N., and Yadav, R.: Contribution of biogenic and photochemical sources to ambient VOCs during
790 winter to summer transition at a semi-arid urban site in India, Environmental pollution, 229, 595-606,
791 10.1016/j.envpol.2017.06.091, 2017.
792 Shao, M., Lu, S., Liu, Y., Xie, X., Chang, C., Huang, S., and Chen, Z.: Volatile organic compounds measured in
793 summer in Beijing and their role in ground-level ozone formation, Journal of Geophysical Research, 114,
794 10.1029/2008jd010863, 2009.
795 Shao, M., Wang, B., Lu, S., Yuan, B., and Wang, M.: Effects of Beijing Olympics Control Measures on Reducing
796 Reactive Hydrocarbon Species, Environ. Sci. Technol., 45, 514-519, 2011.
797 Shao, P., An, J., Xin, J., Wu, F., Wang, J., Ji, D., and Wang, Y.: Source apportionment of VOCs and the contribution to
798 photochemical ozone formation during summer in the typical industrial area in the Yangtze River Delta, China,
799 Atmospheric Research, 176-177, 64-74, 10.1016/j.atmosres.2016.02.015, 2016.
800 Shen, F., Ge, X., Hu, J., Nie, D., Tian, L., and Chen, M.: Air pollution characteristics and health risks in Henan
801 Province, China, Environmental research, 156, 625-634, 10.1016/j.envres.2017.04.026, 2017.
802 Simon, H., Reff, A., Wells, B., Xing, J., and Frank, N.: Ozone trends across the United States over a period of
803 decreasing NOx and VOC emissions, Environmental science & technology, 49, 186-195, 10.1021/es504514z, 2015.
804 Streets, D. G., Fu, J. S., Jang, C. J., Hao, J., He, K., Tang, X., Zhang, Y., Wang, Z., Li, Z., Zhang, Q., Wang, L., Wang,
805 B., and Yu, C.: Air quality during the 2008 Beijing Olympic Games, Atmospheric Environment, 41, 480-492,
806 10.1016/j.atmosenv.2006.08.046, 2007.

807 Sun, J., Wang, Y., Wu, F., Tang, G., Wang, L., Wang, Y., and Yang, Y.: Vertical characteristics of VOCs in the lower
808 troposphere over the North China Plain during pollution periods, Environmental pollution, 236, 907-915,
809 10.1016/j.envpol.2017.10.051, 2018.
810 Tang, J. H., Chan, L. Y., Chan, C. Y., Li, Y. S., Chang, C. C., Liu, S. C., Wu, D., and Li, Y. D.: Characteristics and
811 diurnal variations of NMHCs at urban, suburban, and rural sites in the Pearl River Delta and a remote site in South
812 China, Atmospheric Environment, 41, 8620-8632, 10.1016/j.atmosenv.2007.07.029, 2007.
813 Toro, M. V., Cremades, L. V., and Calbo, J.: Relationship between VOC and NOx emissions and chemical production
814 of tropospheric ozone in the Aburra Valley (Colombia), Chemosphere, 65, 881-888,
815 10.1016/j.chemosphere.2006.03.013, 2006.
816 Tsai, S. M., Zhang, J. J., Smith, K. R., Ma, Y., Rasmussen, R. A., and Khalil, M. A. K.: Characterization of
817 Non-methane Hydrocarbons Emitted from Various Cookstoves Used in China, Environ. Sci. Technol., 37, 2869-2877,
818 2003.
819 U.S.EPA: Revisions to the California state implementation plan and revision to the definition of volatile organic
820 compounds (VOC): removal of VOC exemptions for California's aerosol coating products reactivity-based regulation,
821 Fed. Regist. 70, 53930–53935, 2005.
822 US EPA: EPA Positive Matrix Factorization (PMF) 5.0 Fundamentals and User Guide,
823 http://www.epa.gov/heasd/documents/ EPA. PMF.5.0.User.Guide. pdf, 2014.
824 Wang, H.-l., Jing, S.-a., Lou, S.-r., Hu, Q.-y., Li, L., Tao, S.-k., Huang, C., Qiao, L.-p., and Chen, C.-h.: Volatile
825 organic compounds (VOCs) source profiles of on-road vehicle emissions in China, The Science of the total
826 environment, 607-608, 253-261, 10.1016/j.scitotenv.2017.07.001, 2017a.
827 Wang, H., Qiao, Y., Chen, C., Lu, J., Qiao, L., and Lou, S.: Source Profiles and Chemical Reactivity of Volatile
828 Organic Compounds from Solvent Use in Shanghai, China, Aerosol and Air Quality Research,
829 10.4209/aaqr.2013.03.0064, 2014.
830 Wang, H., Xiang, Z., Wang, L., Jing, S., Lou, S., Tao, S., Liu, J., Yu, M., Li, L., Lin, L., Chen, Y., Wiedensohler, A.,
831 and Chen, C.: Emissions of volatile organic compounds (VOCs) from cooking and their speciation: A case study for
832 Shanghai with implications for China, The Science of the total environment, 10.1016/j.scitotenv.2017.10.098, 2017b.
833 Wang, H. L., Chen, C. H., Wang, Q., Huang, C., Su, L. Y., Huang, H. Y., Lou, S. R., Zhou, M., Li, L., Qiao, L. P., and
834 Wang, Y. H.: Chemical loss of volatile organic compounds and its impact on the source analysis through a two-year
835 continuous measurement, Atmospheric Environment, 80, 488-498, 10.1016/j.atmosenv.2013.08.040, 2013a.
836 Wang, M., Shao, M., Lu, S.-H., Yang, Y.-D., and Chen, W.-T.: Evidence of coal combustion contribution to ambient
837 VOCs during winter in Beijing, Chinese Chemical Letters, 24, 829-832, 10.1016/j.cclet.2013.05.029, 2013b.
838 Wang, M., Shao, M., Chen, W., Lu, S., Liu, Y., Yuan, B., Zhang, Q., Zhang, Q., Chang, C. C., Wang, B., Zeng, L., Hu,
839 M., Yang, Y., and Li, Y.: Trends of non-methane hydrocarbons (NMHC) emissions in Beijing during 2002–2013,
840 Atmospheric Chemistry and Physics, 15, 1489-1502, 10.5194/acp-15-1489-2015, 2015.
841 Wang, T., Xue, L., Brimblecombe, P., Lam, Y. F., Li, L., and Zhang, L.: Ozone pollution in China: A review of
842 concentrations, meteorological influences, chemical precursors, and effects, The Science of the total environment, 575,
843 1582-1596, 10.1016/j.scitotenv.2016.10.081, 2017c.
844 Wang, X.-m., Sheng, G.-y., Fu, J.-m., Chan, C.-y., Lee, S.-C., Chan, L. Y., and Wang, Z.-s.: Urban roadside aromatic
845 hydrocarbons in three cities of the Pearl River Delta, People's Republic of China, Atmospheric Environment, 36, 5141–
846 5148, 2002.
847 Wang, Y., Guo, H., Zou, S., Lyu, X., Ling, Z., Cheng, H., and Zeren, Y.: Surface O3 photochemistry over the South
848 China Sea: Application of a near-explicit chemical mechanism box model, Environmental pollution, 234, 155-166,
849 10.1016/j.envpol.2017.11.001, 2018.

Wei, W., Cheng, S., Li, G., Wang, G., and Wang, H.: Characteristics of ozone and ozone precursors (VOCs and NOx) around a petroleum refinery in Beijing, China, Journal of Environmental Sciences, 26, 332-342, 10.1016/s1001-0742(13)60412-x, 2014.

Wu, R., and Xie, S.: Spatial Distribution of Ozone Formation in China Derived from Emissions of Speciated Volatile Organic Compounds, Environmental science & technology, 51, 2574-2583, 10.1021/acs.est.6b03634, 2017.

Xue, Y., Ho, S. S. H., Huang, Y., Li, B., Wang, L., Dai, W., Cao, J., and Lee, S.: Source apportionment of VOCs and their impacts on surface ozone in an industry city of Baoji, Northwestern China, Scientific Reports, 7, 9979, 10.1038/s41598-017-10631-4, 2017.

Yan, Y., Yang, C., Peng, L., Li, R., and Bai, H.: Emission characteristics of volatile organic compounds from coal-, coal gangue-, and biomass-fired power plants in China, Atmospheric Environment, 143, 261-269, 10.1016/j.atmosenv.2016.08.052, 2016.

Yan, Y., Peng, L., Li, R., Li, Y., Li, L., and Bai, H.: Concentration, ozone formation potential and source analysis of volatile organic compounds (VOCs) in a thermal power station centralized area: A study in Shuozhou, China, Environmental pollution, 223, 295-304, 10.1016/j.envpol.2017.01.026, 2017.

Yuan, B., Shao, M., Lu, S., and Wang, B.: Source profiles of volatile organic compounds associated with solvent use in Beijing, China, Atmospheric Environment, 44, 1919-1926, 10.1016/j.atmosenv.2010.02.014, 2010.

Yuan, B., Hu, W. W., Shao, M., Wang, M., Chen, W. T., Lu, S. H., Zeng, L. M., and Hu, M.: VOC emissions, evolutions and contributions to SOA formation at a receptor site in eastern China, Atmospheric Chemistry and Physics, 13, 8815-8832, 10.5194/acp-13-8815-2013, 2013a.

Yuan, Z., Lau, A. K. H., Shao, M., Louie, P. K. K., Liu, S. C., and Zhu, T.: Source analysis of volatile organic compounds by positive matrix factorization in urban and rural environments in Beijing, Journal of Geophysical Research, 114, 10.1029/2008jd011190, 2009.

Yuan, Z., Zhong, L., Lau, A. K. H., Yu, J. Z., and Louie, P. K. K.: Volatile organic compounds in the Pearl River Delta: Identification of source regions and recommendations for emission-oriented monitoring strategies, Atmospheric Environment, 76, 162-172, 10.1016/j.atmosenv.2012.11.034, 2013b.

Zhang, J., Sun, Y., Wu, F., Sun, J., and Wang, Y.: The characteristics, seasonal variation and source apportionment of VOCs at Gongga Mountain, China, Atmospheric Environment, 88, 297-305, 10.1016/j.atmosenv.2013.03.036, 2014.

Zhang, Z., Wang, X., Zhang, Y., Lu, S., Huang, Z., Huang, X., and Wang, Y.: Ambient air benzene at background sites in China's most developed coastal regions: exposure levels, source implications and health risks, The Science of the total environment, 511, 792-800, 10.1016/j.scitotenv.2015.01.003, 2015.

Zhao, Y., Nguyen, N. T., Presto, A. A., Hennigan, C. J., May, A. A., and Robinson, A. L.: Intermediate Volatility Organic Compound Emissions from On-Road Diesel Vehicles: Chemical Composition, Emission Factors, and Estimated Secondary Organic Aerosol Production, Environmental science & technology, 49, 11516-11526, 10.1021/acs.est.5b02841, 2015.

Zheng, H., Kong, S., Xing, X., Mao, Y., Hu, T., Ding, Y., Li, G., Liu, D., Li, S., and Qi, S.: One year monitoring of volatile organic compounds (VOCs) from an oil-gas station in northwest China, Atmospheric Chemistry and Physics Discussions, 1-57, 10.5194/acp-2017-828, 2017.

Zhu, Y., Yang, L., Kawamura, K., Chen, J., Ono, K., Wang, X., Xue, L., and Wang, W.: Contributions and source identification of biogenic and anthropogenic hydrocarbons to secondary organic aerosols at Mt. Tai in 2014, Environmental pollution, 220, 863-872, 10.1016/j.envpol.2016.10.070, 2017.